Utero-placental expression and functional implications of HSD11B1 and HSD11B2 in canine pregnancy

Miguel Tavares Pereira, Gerhard Schuler, Selim Aslan, Rita Payan-Carreira, Iris Reichler, Karine Reynaud, Mariusz Kowalewski

▶ **To cite this version:**

Miguel Tavares Pereira, Gerhard Schuler, Selim Aslan, Rita Payan-Carreira, Iris Reichler, et al.. Utero-placental expression and functional implications of HSD11B1 and HSD11B2 in canine pregnancy. Biology of Reproduction, 2023, 108 (4), pp.645-658. 10.1093/biolre/ioac214 . hal-04235811

HAL Id: hal-04235811
https://hal.inrae.fr/hal-04235811v1

Submitted on 10 Oct 2023

HAL is a multi-disciplinary open access archive for the deposit and dissemination of scientific research documents, whether they are published or not. The documents may come from teaching and research institutions in France or abroad, or from public or private research centers.

L'archive ouverte pluridisciplinaire **HAL**, est destinée au dépôt et à la diffusion de documents scientifiques de niveau recherche, publiés ou non, émanant des établissements d'enseignement et de recherche français ou étrangers, des laboratoires publics ou privés.

Utero-placental expression and functional implications of HSD11B1 and HSD11B2 in canine pregnancy

Miguel Tavares Pereira[1]; Gerhard Schuler[2]; Selim Aslan[3]; Rita Payan-Carreira[4]; Iris M Reichler[5]; Karine Reynaud[6,7]; Mariusz P Kowalewski[1,8]

[1]Institute of Veterinary Anatomy, Vetsuisse Faculty, University of Zurich (UZH), Zurich, Switzerland
[2]Clinic for Obstetrics, Gynecology and Andrology of Large and Small Animals, Justus-Liebig-University, Giessen, Germany
[3]Department of Obstetrics and Gynecology, Faculty of Veterinary Medicine, Near East University, Nicosia, Cyprus
[4]School of Science and Technology, Department of Veterinary Medicine, University of Évora, Évora, Portugal
[5]Clinic for Reproductive Medicine, Vetsuisse Faculty, University of Zurich (UZH), Zurich, Switzerland
[6]École Nationale Vétérinaire d'Alfort, EnvA, 94700 Maisons-Alfort, France
[7]Physiologie de la Reproduction et des Comportements, CNRS, IFCE, INRAE, Université de Tours, PRC, Nouzilly, France
[8]Center for Clinical Studies (ZKS), Vetsuisse Faculty, University of Zurich (UZH), Zurich, Switzerland

Grant Support

The present work was supported by the Swiss National Science Foundation (SNSF) research grant number 31003A_182481.

Correspondence:
Prof. Dr. Mariusz P. Kowalewski, PhD
Institute of Veterinary Anatomy
Vetsuisse Faculty
University of Zurich
Winterthurerstrasse 260
CH-8057 Zurich, Switzerland
Tel.: 0041-44-6358784; Fax.: 0041-44-6358943
Email: kowalewskipl@yahoo.de or kowalewski@vetanat.uzh.ch

Email addresses:
MTP: miguel.tavarespereira@uzh.ch
GS: Gerhard.Schuler@vetmed.uni-giessen.de
RPC: rtpayan@uevora.pt
SA: selim.aslan@neu.edu.tr
IMR: ireichler@vetclinics.uzh.ch
KR: karine.reynaud@inrae.fr
MPK: kowalewski@vetanat.uzh.ch or kowalewskipl@yahoo.de

Running title

HSD11B1 and -2 expression in the canine placenta

Summary Sentence

The canine placenta appears to have increased trophoblast-mediated inactivation of cortisol during mid-pregnancy, whereas parturition appears to be marked by increased local cortisol availability.

Keywords
dog (*Canis lupus familiaris*), placenta, parturition, cortisol, hydroxysteroid 11-beta dehydrogenase (HSD11B) 1/2

Abstract

Apart from being stress mediators, glucocorticoids modulate the feto-maternal interface during the induction of parturition. In the dog, the prepartum rise of cortisol in the maternal circulation appears to be erratic, and information about its contribution to the prepartum luteolytic cascade is scarce. However, the local placental upregulation of glucocorticoid receptor (GR/NR3C1) at term led to the hypothesis that species-specific regulatory mechanisms might apply to the involvement of cortisol in canine parturition. Therefore, here, we assessed the canine uterine/utero-placental spatio-temporal expression of hydroxysteroid 11-beta dehydrogenase 1 (HSD11B1; reduces cortisone to cortisol), and -2 (HSD11B2; oxidizes cortisol to the inactive cortisone). Both enzymes were detectable throughout pregnancy, their transcriptional levels were elevated following implantation, with a strong increase in *HSD11B2* post-implantation (days 18-25 of pregnancy), and in *HSD11B1* at mid-gestation (days 35-40) (P<0.05).". Interestingly, when compared pairwise, *HSD11B2* transcripts were higher during post-implantation, whereas *HSD11B1* dominated during mid-gestation and luteolysis (P<0.05). A custom-made species-specific antibody generated against HSD11B2 confirmed its decreased expression at prepartum luteolysis. Moreover, in mid-pregnant dogs treated with aglepristone, *HSD11B1* was significantly higher than *-2* (P<0.05). HSD11B2 (protein and transcript) was localized mostly in the syncytiotrophoblast, whereas *HSD11B1* mRNA was mainly localized in cytotrophoblast cells. Finally, in a functional approach using placental microsomes, a reduced conversion capacity to deactivate cortisol into cortisone was observed during prepartum luteolysis, fitting well with the diminished HSD11B2 levels. In particular, the latter findings support the presence of local increased cortisol availability at term in the dog, contrasting with an enhanced inactivation of cortisol during early pregnancy.

1. Introduction

The adrenal-derived cortisol, besides its association with stress, is involved in biological processes including reproductive events such as fetal development and the parturition cascade [1, 2]. Parturition is an orchestrated, mostly species-specific event, involving complex

endocrine signaling cascades that are still not fully characterized in several eutherian species. The sheep is one of the animal species in which the initiation of parturition is well studied and serves as a translational model for other domestic animal species. Thus, in this animal model, parturition appears to be triggered by increased amounts of fetal adrenal-derived cortisol [1, 3], inducing a shift in placental steroidogenic activity towards increased estradiol (E2) production, replacing the local progesterone (P4) production. This leads to increased secretion of placental prostaglandin (PG) F2α, which stimulates myometrial activity [1, 3]. The luteolytic activity of cortisol-induced and placenta-derived PGF2α plays further important roles in species where the corpus luteum is, at least in part, the source of P4, e.g., pig, cow, goat, mouse, cat, and rabbit [4]. Interestingly, in guinea pigs, humans, and other primates, parturition occurs in the presence of high circulating amounts of P4, accompanied, however, by local, i.e., placental, withdrawal of P4 signaling [5-8]. Accordingly, several mechanisms, involving local metabolism, differential expression of P4 receptor (PGR) isoforms, synthesis and availability of lower activity P4 metabolites, and accessibility of transcription factors, have been implied in the underlying regulatory mechanisms [s. reviewed in 7, 9]. In addition, the competitive binding activity observed between the glucocorticoid receptor (GR/NR3C1) and PGR [10, 11] is also thought to contribute to the functional local withdrawal of P4 in human placenta [12]. In contrast, cortisol appears to have a low binding capacity to PGR at physiological levels [10, 13].

The unique endocrinological features of the dog, when compared with other domestic mammals, hinder the translation of different parturition-associated biological strategies observed in other species. The dog is the only domestic mammal in which no steroidogenic activity is observed in the placenta, with P4 being produced solely by the corpus luteum (CL) [14, 15]. This further accounts for the absence of a parturition-specific increase of estrogens [14, 16]. Furthermore, due to the absence of anti-luteolytic mechanisms during early diestrus, the dog presents an inherently regulated and long lasting activity of the CL [17, 18]. In the canine endotheliochorial placenta, maternal stroma-derived decidual cells are the only cellular population expressing the nuclear PGR [19-21]. This distribution of PGR is especially important when considering the parturition cascade. The prepartum decline of circulating P4 levels, or functional blocking of PGR with antigestagens (e.g., aglepristone), results in decreased decidual cell-mediated P4/PGR signaling, associated with increased prepartum production of luteolytic PGF2α by the trophoblast, and leading to parturition/abortion [22].

Regarding canine cortisol, increased circulating amounts have been reported in dogs at the time of parturition [14, 23-25]. However, due to wide variation in detected levels, ranging from nadir

to clearly measurable values, elevated circulating cortisol levels are not considered a prerequisite for the induction of parturition in dogs and could be indicative of maternal stress [14, 23]. Nevertheless, despite its weak clinical applicability (repeated treatments with high dosages over longer time, associated with strong side effects), the termination of canine pregnancy can be induced with exogenously-administered glucocorticoids during the last third of pregnancy [26-28]. Furthermore, GR/NR3C1 was detected in the canine fetal trophoblast, and was upregulated in the placenta at the time of prepartum luteolysis [29]. Interestingly, in samples collected after preterm induction of luteolysis with aglepristone, GR/NR3C1 expression remained unaffected, despite the increased PGF2α output observed following treatment [21]. Jointly, these observations exclude the increased availability of GR/NR3C1 as a requirement for the prepartum release of PGF2α in the dog [29]. Instead, it was proposed that GR/NR3C1 could be involved in a P4 withdrawal mechanism [29], similar to its proposed role in humans [12].

Underlying the present project, we hypothesized that glucocorticoids might be involved in the parturition cascade in the dog, and that their signaling and availability might be regulated locally in the placenta. Accordingly, recently, changes in the placental transcriptional profile during parturition were investigated in canine placental samples collected during mid-pregnancy and at the time of luteolysis, both prepartum and antigestagen-induced (abortion at mid-term) [30]. Among the differentially expressed genes were factors identified as potentially modulated by P4, i.a., hydroxysteroid 11-beta dehydrogenase 2 (*HSD11B2*), that, although being initially abundantly expressed, was downregulated during the termination of pregnancy [30]. HSD11B2, together with HSD11B1, interconvert the biologically inactive cortisone and the active cortisol [31]. HSD11B1 is predominantly a reductase, reducing cortisone into cortisol, and is expressed in several tissues (e.g., liver, adipose tissue and placenta, central nervous system, cardiovascular system or immune system), where it increases the intracellular glucocorticoid availability [31, 32]. Moreover, HSD11B1 can act as a dehydrogenase under specific circumstances, mainly associated with the disruption of cellular activity and/or metabolic disturbances like diabetes or obesity [31, 32]. In contrast, HSD11B2 acts solely as a dehydrogenase, decreasing local cortisol availability by converting it into cortisone [31]. The cortisol-inactivating function of HSD11B2 in the placenta acts as a protective mechanism against the passage of glucocorticoids into fetal circulation in humans [33]. However, the only information to date about these factors in the canine placenta is from the transcriptomic study [30]. To contribute to the knowledge regarding local regulatory mechanisms, and test our hypothesis regarding the local involvement of cortisol metabolism in the maintenance of canine

pregnancy, we investigated the expression and regulation of HSD11B1 and -2 in the canine uterus and/or placenta throughout pregnancy.

2. Materials and Methods

2.1 Tissue collection and preservation

Uterine/utero-placental samples from 41 clinically healthy crossbred sexually mature bitches were collected by routine ovariohysterectomy. Several of these tissue samples originated from previous studies, where details on animal manipulation and staging of pregnancy are described [21, 30, 34-37]. Animal experiments were carried out in accordance with animal welfare ethical principles and legislation, and approved by the responsible ethics committees of the Justus-Liebig University Giessen, Germany (permits no. II 25.3-19c20- 15c GI 18/14 and VIG3-19c-20/ 15 GI 18,14); of the University of Ankara, Turkey (permits no. Ankara 2006/06 and 2008–25– 124); and of the national review board CNREEA #16 (APAFIS #2015042112442132) for the Alfort Veterinary School (facility 947-046-2), France. Further samples from animals submitted to routine ovariohysterectomy at the Section of Small Animal Reproduction, Vetsuisse Faculty, Zurich, were collected after the owners' informed consent.

The onset of spontaneous estrus was observed in all animals, with the day of ovulation being determined when circulating P4 concentration exceeded 5 ng/ml. After the required period for oocyte maturation in the oviduct, i.e., 2-3 days [17], animals were mated (day 0 of pregnancy). Uterine or utero-placental samples (depending on the pregnancy stage) were divided in the following groups: non-pregnant animals (E-, days 8 - 12 after mating, n = 5), pre-implantation (E+, days 8 - 12 of pregnancy, n = 5), time of implantation (Day 17, n = 4), post-implantation (Post-Imp, days 18 – 25 of pregnancy, n = 7), mid-gestation (Mid-Gest, days 35 - 40 of pregnancy, n = 6), prepartum luteolysis (Lut, n = 4), 24h after aglepristone treatment (Agle 24h, n = 5) and 72h after aglepristone treatment (Agle 72h, n = 5). As implantation takes place at day 17 [20, 38, 39], confirmation of pregnancy during early pre-implantation period was performed with embryo flushing (E+). Animals in which no embryos could be retrieved between days 8 - 12 were allocated to the non-pregnant control group (E-). Samples from the Lut group were collected during active prepartum P4 decline, determined by hormonal measurements every 6h until P4 concentrations were below 3 ng/ml in three consecutive assessments. Aglepristone (Alizine, Virbac, Bad Oldesloe, Germany) was used to induce the termination of pregnancy in 10 animals at mid-pregnancy (days 40 – 45 after mating), following the protocol provided by the supplier, i.e., administration of 10 mg/kg body weight twice 24h

apart. Samples containing uterine and placental sections were collected 24 or 72h after the second administration of aglepristone.

After surgery, samples were washed with PBS and dissected from connective tissue. Samples used for RNA and protein analysis were immersed in RNAlater (Ambion Biotechnology GmbH, Wiesbaden, Germany) at 4ºC for 24h and then stored at -80ºC until needed. For histology, samples were fixed in 10% phosphate-buffered formalin for 24h, washed with PBS for 7 consecutive days, dehydrated in an ethanol series, transferred into xylol and embedded in paraffin. Whereas all samples were used for TaqMan PCR, 3 samples/group were used for immunohistochemistry and *in situ* hybridization experiments.

2.2 RNA isolation, reverse transcription and semi-quantitative real-time TaqMan PCR

The isolation of total RNA was performed with TRIzol reagent (Invitrogen, Varlsbad, CA, USA), following the supplier's instructions. A NanoDrop 2000 spectrophotometer (ThermoFisher Scientific AG, Reinach, Switzerland) was used to assess RNA quantity and purity. For each sample, RNA was cleaned of possible contaminating genomic DNA with the RQ1 RNA-free DNase kit (Promega, Dübendorf, Switzerland), and reverse transcribed using the MultiScribe Reverse Transcriptase with random hexamers used as primers (Applied Biosystems by Thermo Fisher, Foster City, CA, USA); cDNA corresponding to 1.2µg of total RNA was used per sample and reaction. The relative gene expression was assessed by semi-quantitative real time TaqMan PCR, following the previously described protocol [40, 41], in an ABI PRISM 7500 Sequence Detection System fluorometer (Applied Biosystems). All reactions were run in duplicate with Fast Start Universal Probe Master (Roche Diagnostics AG, Basel, Switzerland) and gene expression TaqMan assays targeting *HSD11B1* (Cf02626817_m1) and *HSD11B2* (Cf02690463_s1), all obtained from Applied Biosystems. Autoclaved water and non-reverse transcribed DNase-treated RNA were used as negative controls. Relative quantification was performed with the comparative Ct method (ΔΔCt), following logarithmic transformation of values, calibrated to the average expression among all samples, and normalized to the expression of reference genes. Initially, three reference genes were evaluated, following our recent description [42]: *PTK2* (Cf02684608_m1), *EIF4H* (Cf02713640_m1) and *KDM4A* (Cf02708629_m1). The evaluation of the stability of the reference genes was further assessed with RefFinder [43]. Since PTK2 and KDM4A were more stable than EIF4H in the samples used in this study, these two genes were used for the ΔΔCt calculation.

For the compartmentalization studies, formalin-fixed and paraffin-embedded (FFPE) utero-placental samples from 3 animals belonging to Mid-Gest or Lut groups were used, according to our previously described protocol [29, 44]. A total of 3 tissue sections per animal were cut with 5 μm thickness and mounted on Arcturus PEN membrane glass slides (LCM0522, Applied Biosystems). Tissue sections were then deparaffinized, rehydrated, stained with hematoxylin for histological visualization and dried overnight at 37ºC. Using a stereomicroscope, the different utero-placental compartments (i.e., placental labyrinth, endometrium and myometrium) were identified and dissected with sterile scalpel blades. Total RNA was isolated using the RNeasy FFPE Kit (Qiagen GmBH, Hilden, Germany), following the manufacturer's protocol, and RNA concentration was measured with a NanoDrop 2000. Following the variable, and sometimes low, yield of RNA obtained from these samples (ranging 43 to 416 ng/μl), 10 ng of RNA were DNase treated and reverse transcribed with the High Capacity cDNA Reverse Transcription Kit (Applied Biosystems). Afterwards, the obtained cDNA was amplified with the TaqMan PreAmp Master Mix kit, following the supplier's protocols and as previously described [40]. For this, TaqMan assays for *HSD11B1*, *HSD11B2* and reference genes were pooled and mixed with the previously prepared cDNA and TaqMan Preamp Master Mix. Samples were then amplified using an Eppendorf Mastercycler (Vaudax-Eppendorf AG, Basel, Switzerland). Following this, the semi-quantitative PCR and relative gene expression quantification was performed as described above.

2.3 Immunohistochemistry (IHC)

Since no species-specific or cross-reacting antibodies were commercially available for the canine species, the development of polyclonal antibodies was attempted, as previously described [44], and was successful for generating a custom-made anti-HSD11B2 antibody (but not for HSD11B1) (Eurogentec Seraing, Belgium). Therefore, guinea pigs were immunized using the peptide sequence C+RALRPGQPGSTPAQ (aa 270-284) and C+LAAQPRRRYYPGRGL (aa226-240), based on the available sequences (GenBank accession number XM_005620822.3). Cysteine (C+) was added to the N-terminal to allow peptide conjugation to carrier proteins, and the NH2-terminus was added to the C-end of the peptide to mimic the uncharged peptide bond in the protein. After preliminary assessments of IHC staining, the affinity purified antibody targeting the sequence C+RALRPGQPGSTPAQ was used in further analyses.

The standard indirect immunoperoxidase method was used for IHC to localize the expression of HSD11B2 protein in the canine placenta during post-implantation, mid-gestation and

prepartum luteolysis. Additionally, to allow for better differentiation between cell types, consecutively cut slides from mid-gestation animals were stained against the endothelin receptor B (goat polyclonal anti-EDNRB, sc-21196, Santa Cruz Biotechnology), staining for syncytiotrophoblast [45], and nuclear progesterone receptor (mouse monoclonal anti-PGR, IM1408, Beckman Coulter Life Sciences, Indianapolis, IN, USA), staining for decidual cells [21]. IHC was performed as previously described [40, 41]. Sections with 3 µm of FFPE tissue samples were mounted on microscope slides (SuperFrost; Menzel-Glaeser, Braunschweig, Germany), deparaffinized and rehydrated. Antigen retrieval was performed by heating in a microwave oven with Tris-EDTA buffer (10mM Tris base + 1mM EDTA solution, pH = 9, for HSD11B2) or 10mM citrate buffer (pH = 6, for PGR and EDNRB). After quenching endogenous peroxidase activity with 0.3% hydrogen peroxidase in methanol, slides were incubated in 10% goat or horse serum (depending on the secondary antibody) to decrease nonspecific binding, and then incubated overnight at 4ºC with primary antibodies at the following dilutions: anti-HSD11B2 diluted at 1:1000; anti-PGR at 1:100.; EDNRB at 1:200. Pre-immune serum (in the case of HSD11B2) or non-immune IgG (in the case of PGR and EDNRB) were used as negative/isotype controls (goat IgG I-5000, and mouse IgG I-2000, both from Vector Laboratories Inc., Burlingame, CA, USA), at the same protein concentration as the primary antibodies. Following the incubation with a biotinylated secondary antibody diluted at 1:100 (BA-7000 goat anti-guinea pig for HSD11B2; BA-9500 horse anti-goat IgG for EDNRB; BA-2000 horse anti-mouse IgG for PGR; all from Vector Laboratories Inc.) and with streptavidin-peroxidase ABC kit (Vector Laboratories Inc.), positive signals were revealed with the Liquid DAB+ substrate kit (Dako Schweiz AG, Baar, Switzerland). Slides were then counterstained with haematoxylin, dehydrated and mounted with Histokit (Assistant, Osterode, Germany). The localization of positive signals and capture of representative pictures were performed with a Leica DMRXE light microscope equipped with a Leica Flexacam C1 camera (Leica Microsystems, Wetzlar, Germany).

2.4 *In situ* hybridization (ISH)

As the coding sequence available for canine *HSD11B2* in GenBank was only predicted, molecular cloning was performed to confirm the sequence and generate templates for cRNA to be used in ISH. Therefore, the following primers were used: forward: 5'-CCA AGA AGC TAG ATG CCA TG-3', reverse: 5'-CCT GTG GGC ACT GCT CAT T-3' (ordered from Microsynth AG, Balgach, Switzerland), generating amplicons of 937 bp. Hot start PCR was applied with AmpliTaq Gold DNA polymerase (Applied Biosystems) using two uterine cDNA samples;

annealing temperature was set at 58ºC. PCR products were separated on a 2% agarose gel stained with ethidium bromide and isolated using the QIAquick Gel Extraction Kit (Qiagen GmBH). The products were then subcloned into pGEM-T vector (Promega) before transforming into XL1 Blue competent cells (Stratagene, La Jolla, CA, USA) for multiplication. Plasmids were isolated with the PureYield Plasmid Miniprep System (Promega), and control double-digestion was performed with NcoI and NotI restriction enzymes (New England Biolabs, Frankfurt, Germany). Plasmids were then sent for commercial sequencing (Microsynth AG). The partial sequence of canine-specific *HSD11B2* was submitted to GenBank with the accession number.

In the next step, the cellular localization of transcripts encoding for both enzymes was assessed with non-radioactive ISH, following our previously published protocols [21, 46, 47]. Placentae collected during mid-gestation and prepartum luteolysis were used. In addition to the cloned sequence of *HSD11B2* that was used as a template for generating riboprobes, the canine-specific *HSD11B1* sequence was available in GenBank: NM_001005756.1. The following primers were then used for both targets; *HSD11B1* for: 5'-GCA GAA GCA TGG AAG TCA AC-3', rev: 5'-TGA GGC CGA GGA TAC AGA G-3', 251 bp; and *HSD11B2* for: 5'- ACC TCA GCC CAG TCG TAG AT-3', rev: 5'- AGG GCC TTC ATT TGG ATC TGG -3', 248bp (ordered from Microsynth). The PCR products were then purified and subcloned into pGEM-T plasmids following the protocol described above. The specificity and identification of sense and anti-sense direction of products in the plasmid was performed by commercial sequencing of plasmids single cut with either NcoI or NotI restriction enzymes (Microsynth AG), and cRNA probes labelled with digoxigenin (DIG) were synthetized using the DIG-RNA Labelling Kit (Roche Diagnostics AG). The efficiency of riboprobes synthesis was confirmed with a dot-blot analysis, evaluating signal intensity in serial dilutions of the probes in positively charged nylon membranes stained against DIG (Roche Diagnostics AG). In the next step, tissue sections of 2 µm thickness were mounted on microscope slides, deparaffinized in xylene, rehydrated, digested with 70 µg/ml proteinase K for 19 mins at 37ºC (Sigma-Aldrich Chemie GmbH) and post-fixed with 4% paraformaldehyde. *In situ* hybridization of cRNA probes was performed overnight at 37ºC in the presence of formamide. Sense probes served as negative controls. After blocking of nonspecific signals with 3% ovine serum, samples were incubated overnight with alkaline phosphatase-conjugated sheep anti-DIG Fab Fragments diluted 1:5000 (Roche Diagnostics AG). Endogenous alkaline phosphatase signals were blocked with levamisole. Detection of positive signals was performed with 5-bromo-4-chloro-3-indolyl phosphate and nitroblue tetrazolium (BCIP/NBT, Roche Diagnostics AG). Representative pictures were

obtained with a Leica DMRXE light microscope equipped with a Leica Flexacam C1 camera (Leica Microsystems).

2.5 Protein extraction and western blot

The relative protein expression of HSD11B2 was assessed, following our previously published protocols [35, 48]. Randomly selected utero-placental samples from post-implantation, mid-gestation and prepartum luteolysis groups (n = 3/group) were homogenized in lysis buffer (Net2 Buffer: 50 mM Tris–HCl, pH = 7.4, 300 mM NaCl, 0.05% NP-40; containing 10µl/ml of protease inhibitor cocktail) on using an IKA Euro-ST D overhead stirrer (IKA-Werke GmbH, Staufen, Germany). Samples were then centrifuged (10 min at 10,000 *g*) and the protein content of the supernatants was then quantified with the Bradford assay using a SmartSpec Plus spectrophotometer (Bio-Rad Laboratories, Munich, Germany). Protein samples were normalized with a sample buffer (25 mM Tris-Cl, pH = 6.8, containing 1% SDS, 5% β-mercaptoethanol, 10% glycerol and 0.01% bromophenol blue), and 20 µg of protein from each sample were heated at 95ºC for 10 min, followed by electrophoresis separation in a 10% polyacrylamide gel (AppliChem GmBH, Darmstadt, Germany). Proteins were then transferred into a methanol-activated polyvinylidene difluoride (PVDF) membrane (Bio-Rad Laboratories). Non-specific binding sites were blocked with 5% low-fat powdered milk diluted in PBST (PBS + 0.25% Tween-20), and membranes were incubated overnight at 4ºC with anti-HSD11B2 antibody diluted at 1:250 in 2.5% low-fat powdered milk in PBST solution. Membranes were then incubated with a rabbit anti-guinea pig horseradish peroxidase (HRP)-conjugated antibody (1: 15000, A5545, Sigma Aldrich Chemie GmbH, Buchs, Switzerland), followed by the detection of signals with the SuperSignalWest Chemiluminescent Kit substrate (Thermo Fisher Scientific AG, Reinach, Switzerland) in a Chemi-Doc XRS+ System and Image Lab Software (Bio-Rad Laboratories). To ensure specificity, anti-HSD11B2 antibody was incubated for 1h at ambient temperature with the immunization peptide (blocking peptide) at the same dilution, before being used to blot the membrane. For loading control and relative quantification, PVDF membranes were re-blotted with mouse monoclonal antibody against ACTINB (1:1000, sc-69879, Santa Cruz Biotechnology, Santa Cruz, CA, USA), followed by a goat anti-mouse HRP-labelled secondary antibody (1: 15000, W402B, Promega). The optical density of bands was measured with ImageJ software (US National Institutes of Health, Bethesda, Maryland, USA). Relative protein expression was calculated by normalizing the optical density of HSD11B2 against ACTINB in the reblotted membranes and is presented as standardized optical density (SOD).

2.6 Evaluation of uteroplacental cortisol-cortisone conversion capacity

To evaluate the capacity of placental tissue to interconvert cortisol and cortisone, microsomal fractions (crude endoplasmic reticulum) were isolated from utero-placental sections collected during the post-implantation period, as well as from placenta and endometrium, and myometrial samples (macroscopically dissected) at the time of prepartum luteolysis (n = 4/group). This was done using the Endoplasmic Reticulum Isolation Kit (Sigma Aldrich Chemie GmbH), according to the manufacturer's directions and as previously described [49].

All conversion capacity assays were performed blinded, using incubation protocols modified after [49, 50]. Reaction mixtures (100 µl volume) were created by combining 50 µl of microsomal fractions with co-factors and substrates. For the cortisol to cortisone conversion assay, 0.25 mM NAD^+ (Roche Diagnostics, Mannheim, Germany) was used as co-factor, and substrate was 25 nM of unlabeled cortisol (Merk KGaA, Daarmstadt, Germany) and 1.82 nM (20 000 cpm) of tritium-labeled [1,2,6,7-3H(N)]-cortisol (PerkinElmer LAS GmbH, Rodgau, Germany). For the cortisone to cortisol conversion assay, the co-factor was 0.25 mM NADPH $+H^+$ (Roche Diagnostics), while the substrates were 25 nM of unlabeled cortisone (Merk KGaA) and 7.5 nM (60 000 cpm) of tritium-labeled [1,2-3H(N)]-cortisone (PerkinElmer LAS GmbH). The use of a mixture of unlabeled and 3H-labeled substrates was performed to minimize radioactive waste, while still allowing the evaluation of conversion rates. Mixtures using random samples were initially incubated for 0, 5, 10, 20 and 30 mins at 37ºC to determine the ideal incubation time. An incubation time of 20 mins was considered the most suitable time by showing the maximal conversion capacity of the mixture, and was then used for all subsequent experiments. After incubation was complete, samples were extracted with ethyl acetate, dried in a MicroDancer infrared vortex-evaporator (Hettich AG, Baech, Switzerland) and redissolved in 100 µl of HPLC mobile phase (methanol/acetonitrile/water 43:3:54 v/v/v). Samples were then separated via HPLC, following the protocol described in [51]. In short, 20 µl of dissolved extracts were separated on a 150 × 4 mm Eurospher II 100-5 C18 reversed-phase column in a Smartline Manager 5050 and Pump 150 HPLC system (all HPLC equipment from Knauer, Berlin, Germany) at a flow rate of 1 mL/min. Eluted fractions with 0.5 ml were then collected and evaporated. The 3H-activity in HPLC fractions was then measure by adding the scintillation cocktail Rotiszint eco plus (Carl Roth GmbH, Karlsruhe, Germany) in a Tri-Carb 2810 TR β-scintillation counter (PerkinElmer LAS GmbH). Differentiation between substrate and metabolite was based on a comparison of retention times with authentic tritiated standards. The percent of substrate conversion was calculated from the distribution of 3H activity among

the peaks after subtracting technical background of β-scintillation counter and baseline correction.

2.7 Statistical analysis

Statistical evaluation of changes in relative transcript levels (relative gene expression, RGE) and protein amounts (standardized optic density, SOD) between different stages of pregnancy was performed by one-way ANOVA, followed by Tukey-Kramer multiple comparisons post-test. In addition, two-tailed unpaired Student's t-test was performed to evaluated possible differences in pairwise comparisons, i.e. between mRNA amounts of *HSD11B1* and *-2* in different groups. The software GraphPad 2.06 (GraphPad Software Inc, San Diego, CA, USA) was used for this analysis and $P < 0.05$ was considered as statistically significant.

3. Results

3.1 Uterine/utero-placental gene expression during pregnancy

The transcriptional availability of *HSD11B1* and *-2* was evaluated in all uterine/utero-placental tissue samples. The mRNA availability of *HSD11B1* was significantly higher at mid-gestation, when compared with all earlier stages of pregnancy, and non-pregnant (E-) uterine samples ($P < 0.001$, Fig. 1A). There was a high variation in *HSD11B1* expression during luteolysis, yielding no significant difference between mid-gestation and luteolysis ($P > 0.05$, Fig. 1A). Yet, in antigestagen-induced luteolysis/abortion, the expression of *HSD11B1* was significantly increased 24 h after mid-pregnant animals were treated with aglepristone ($P < 0.05$, Fig. 1B). The availability of *HSD11B2* mRNA was the highest in post-implantation and mid-gestation samples, when compared with all other evaluated stages ($P < 0.05$, Fig. 1C). In contrast with *HSD11B1*, the expression of *HSD11B2* was downregulated in samples collected 24 and 72 h after aglepristone treatment ($P < 0.05$, Fig. 1D), resembling the pattern observed during normal luteolysis. In a pairwise comparison of both enzymes in canine uterine and utero-placental samples, *HSD11B2* expression was significantly higher than *-1* during post-implantation ($P < 0.001$, Fig. 1E). This changed during mid-gestation and prepartum luteolysis, with *HSD11B1* transcripts being more abundant than *HSD11B2* ($P < 0.01$ and $P < 0.05$, respectively, Fig. 1E). A higher expression of *HSD11B1* than *HSD11B2* was further observed in animals treated with aglepristone ($P < 0.01$, Fig. 1F).

3.2 Compartmentalization of *HSD11B1* and *-2* mRNA in the canine uterus

The mRNA abundance of all factors in different tissue layers, i.e., placental labyrinth, endometrium or myometrium, was assessed in utero-placental units collected during mid-gestation (i.e., in the mature fully developed placenta) and prepartum luteolysis. The availability of both *HSD11B1* and *HSD11B2* transcripts was frequently below detection limits in the myometrium of animals at mid-gestation resulting in the exclusion of these samples from the statistical evaluation. (Fig. 2). Due to high individual variability, no significant differences were observed for the expression of *HSD11B1* between the tissue compartments at mid-gestation ($P > 0.05$). This contrasted with its expression during prepartum luteolysis, with the placenta showing significantly higher levels than endometrium or myometrium ($P < 0.05$, Fig. 2A), suggesting the placenta as being the major source. *HSD11B2* transcripts were significantly more abundant in the mid-gestation placenta compared with mid-gestation endometrium ($P < 0.01$), and with the placental labyrinth and myometrium of prepartum luteolysis ($P < 0.001$ and $P < 0.01$, respectively, Fig. 2B). Furthermore, endometrial availability of *HSD11B2* was significantly higher than in the placenta during prepartum luteolysis ($P < 0.05$, Fig. 2B).

3.3 Protein expression of HSD11B2 in the canine utero-placental unit

The canine-specific anti-HSD11B2 antibody allowed the detection of a band close to the predicted protein size (44kDa) in western blot analysis (Fig. 3A). The signal was quenched with antibody pre-incubated with the immunization peptide (Fig. 3A). In utero-placental homogenates, HSD11B2 protein expression was significantly higher at post-implantation than mid-gestation and prepartum luteolysis ($P < 0.01$ and $P < 0.001$, respectively, Fig. 3B), mirroring the time-dependent changes observed at the mRNA level.

3.4 Localization of HSD11B1 and HSD11B2 in the canine placenta

The availability of custom-made anti-HSD11B2 antibody has made it possible to study its expression at both the protein and RNA level, whereas the localization of HSD11B1 was possible only by applying ISH.

During post-implantation, HSD11B2 was predominantly localized at the embryo-maternal interface of the developing placenta, in invading cytotrophoblast cells (Fig. 4A, left panels). In the mature placenta, during mid-gestation, signals were mostly localized in the syncytiotrophoblast, with some weaker staining in other cellular components (e.g. decidual cells or endothelial cells (Fig. 4A, center panels)). At prepartum luteolysis, the signals were weaker and a more diffuse staining pattern was observed (Fig. 4A, right panels). The

localization of HSD11B2-positive signals in the syncytiotrophoblast was then confirmed in the mature placenta by performing staining of consecutive slides (Fig. 4B) against PGR, as a marker of decidual cells [19, 20], and EDNRB, expressed by the syncytiotrophoblast [45].

With ISH, positive signals for *HSD11B1* were mostly localized in cytotrophoblast cells, with some signals also observed in maternal endothelial cells (Fig. 5A), while for *HSD11B2*, the signals were mainly observed in the syncytiotrophoblast, with a more diffuse pattern observed during luteolysis than during mid-gestation, as seen with IHC (Fig. 5B).

3.5 Enzymatic conversion between cortisol and cortisone in canine placental homogenates

The potential of the placenta to interconvert cortisol and cortisone was evaluated in samples collected during post-implantation, where a significantly higher mRNA availability of *HSD11B2* than *-1* was observed, and at the time of prepartum luteolysis, where an inverted pattern, associated with decreased protein expression of HSD11B2, was observed. Due to difficulties in the separation of intact tissue layers containing the invading trophoblast from remaining tissue layers in the still developing utero-placental interface at post-implantation, full tissue cross-sections were used for post-implantation specimens. On the other hand, in the fully developed placenta at prepartum luteolysis, the separation between physiological layers of placenta with adjacent endometrium from myometrium (the latter presenting low mRNA availability of both factors, being used as a negative control) was performed at the level of physiologically significantly enlarged endometrial chambers (i.e., deep endometrial glands). When evaluating conversion rates, values below 5% were considered as unreliable, as the presence of impurities or decay of the cortisol tracer, in addition to possible technical background of the beta counter, can mask weak conversion effects.

The conversion of cortisol into cortisone (i.e., inactivation of cortisol, indicating HSD11B2 activity), was significantly higher in utero-placental samples collected at post-implantation, when compared with the conversion rate observed with microsomes isolated from either the placenta or myometrium obtained during prepartum luteolysis ($P < 0.05$, Fig. 6). In contrast, the conversion of cortisone into cortisol (i.e., activation of cortisol) was undetected in post-implantation samples and myometrium from luteolysis, or remained below 1% in placental + endometrium samples collected during luteolysis (not shown).

4. Discussion

In the attempt to gain new insights into the utero-placental availability of cortisol in the dog, we evaluated the expression and localization of cortisol-to-cortisone interconverting enzymes

HSD11B1 and -2 in the canine uterus and utero-placental compartments throughout pregnancy. Both cortisol-regulating enzymes were expressed in all samples. Based on their significantly lower uterine expression at the pre-implantation stage (E+) and in corresponding non-pregnant controls (E-), as well as on the day of implantation (day 17), than in later gestational stages, they appeared to be predominantly associated with placental development and functionality. Therefore, subsequent analyses focused mainly on stages of pregnancy in which a placenta was present, i.e., post-implantation, mid-gestation and prepartum luteolysis. Indeed, *in situ* hybridization analysis of both factors, and immunohistochemical detection of HSD11B2, localized both enzymes predominantly to the fetal-derived trophoblast cells within the canine placental labyrinth.

The transcriptional availability of *HSD11B1* was the highest at mid-gestation, while *HSD11B2* mRNA levels were already increased during post-implantation. Therefore, there seemed to be a higher transcriptional availability of *HSD11B2* than *HSD11B1* associated with early placentation (post-implantation). An excessive exposure to glucocorticoids can cause detrimental effects in the establishment of pregnancy and in fetal development in different species [33, 52, 53]. Several of these effects are associated with disrupted expression of HSD11B2 [54, 55]. Thus, the cortisol-inactivating capacity of HSD11B2 has been characterized as a protective barrier against the passage of glucocorticoids into fetal circulation [33, 56-58]. In humans, e.g., fetal glucocorticoids are 5-10 times lower than maternal circulatory levels [59]. Although several studies have attempted to measure fetal exposition to cortisol in the dog using, e.g., puppy hair and claws [60, 61], a clear comparison with maternal levels is still not available. Nevertheless, it appears plausible that such a protective mechanism might be present in the dog, too. This hypothesis appears to be further supported by the microsomes activity assay, where an increased conversion of cortisol into cortisone was observed in post-implantation samples when compared with luteolysis. With regard to the post-implantation group, the high variability might be due to individual variations or to time-dependent changes. Nevertheless, there is a clearly higher capacity for cortisol inactivation (conversion to cortisone) during post-implantation than at the prepartum luteolysis. Within the fully developed fetal placental compartment, the strongest HSD11B2-positive signals were mainly localized in the syncytiotrophoblast. A similar localization pattern was previously described in mice, with placental HSD11B2 being mainly associated with the trophoblast [62], as well as in humans, where it was exclusively detected in the syncytiotrophoblast [58, 63]. Interestingly, in sheep, representing a non-invasive type of placentation, *HSD11B2* could be detected reliably in the trophectoderm and endoderm of the conceptus, but not in the uterus,

during early pregnancy [64]. Thus, despite the weak signals observed in endothelial and decidual cells in the present study, the increased cortisol-deactivation, possibly associated with a protective embryonal mechanism against maternal cortisol, appears to be mainly mediated by the trophoblast during early fetal development.

The progression of pregnancy towards parturition was associated with a decreased utero-placental expression of HSD11B2, which was confirmed at both the mRNA and protein levels. This was also reflected in its low activity at prepartum luteolysis based on the microsomal cortisol conversion rates. In fact, with average conversions of 2% in the placenta and endometrium, and 1.9% in myometrium (both below the defined 5% threshold), luteolysis appears to be virtually devoid of cortisol into cortisone conversion activity. The decreased placental availability of HSD11B2 at term was also highlighted by the assessment of mRNA in different utero-placental compartments, showing its significantly lowered levels between fully developed mid-term placenta and prepartum luteolysis. Fitting with these observations was the lowered *HSD11B2* transcription in antigestagen-treated dogs, emphasizing the P4-dependent expression of HSD11B2. This supports our previous report using the transcriptomic approach [30], where *HSD11B2* was described as a downstream factor from P4 signaling. As several samples used in the present work derived from previous projects, serum samples that could allow a correlation between placental expression of HSD11B1/2 and circulating cortisol or P4 were not available. Nevertheless, circulating P4 levels are described to a greater extent in the dog [s. reviewed in 65]. Thus, the time-dependent decrease of HSD11B2 expression appears to accompany, at least in part, the decreasing P4 circulating levels observed in this species, including the steep prepartum decline. In ovariectomized mouse, the uterine expression of *HSD11B2* could be upregulated by P4 administration, and later ablated by the PGR blocker mifepristone (RU486) [57]. Aglepristone used in our studies is a derivate of mifepristone, both type II antigestagens, with similarities in its chemical structure and activities related to the PGR [66]. Cumulatively, the recently postulated association between P4/PGR signaling and placental *HSD11B2* expression in the dog [30], is substantiated by the present findings, clearly indicating its importance in the luteolytic cascade.

The diffuse staining of HSD11B2 in the prepartum labyrinth could possibly be associated with its significantly lowered abundance and/or degradation. Conversely, the utero-placental availability of *HSD11B1* increased from post-implantation to mid-gestation, and remained unaffected at prepartum luteolysis. This was associated with an apparent shift in the transcriptional availability of both isoforms, with *HSD11B1* being significantly higher than -*2* at term. The ISH allowed the detection of mRNA encoding for *HSD11B1* mainly in the

cytotrophoblast, with some signals also identified in maternal endothelial cells during prepartum luteolysis These observations suggest that a possible interplay between the cortisol-deactivating syncytiotrophoblast and cortisol-activating cytotrophoblast could be present in the canine placenta. For instance, in mice, increased expression of *HSD11B1* can be observed in late pregnancy in fetal tissue [62], and in humans it is localized in endothelial cells and different trophoblast populations, but not in the syncytiotrophoblast [67]. As part of the approach involving microsomal activities, we investigated the potential of the placenta to activate cortisol, thereby addressing the activity of HSD11B1, which was below reliable detection limits in the placenta from prepartum luteolysis, and was undetectable in myometrium and in post-implantation samples. The inclusion of a positive control tissue, which was not possible in this study, could provide a more definitive answer regarding the lack of cortisol activation. While the low detection of HSD11B1 activity, and the limitations in protein detection, could be explained by a low availability of this enzyme in the canine placenta, this remains to be confirmed. The higher utero-placental transcriptional availability of *HSD11B1* in the antigestagen treated dogs differed from that observed during normal parturition. A possible explanation could be in the local stress-related response to acute PGR withdrawal [s. reviewed in 66]. Despite the still veiled importance of the parturition-associated increase of cortisol activity in the dog, as mentioned elsewhere, the cortisol-stimulated shift in placental steroidogenesis described for other species [1, 3], does not apply to the dog [14, 15]. Furthermore, only term, and not aglepristone-induced termination of pregnancy, was associated with the upregulation of GR/NR3C1 [29]. Nevertheless, the lower HSD11B2 activity appears to be associated with a locally increased availability of cortisol, possibly embryo-derived. This local cortisol increase could be an important event in the final maturation of the fetus, associated, e.g., with the final maturation of fetal organs, like the lung [68]. Still, the confirmation of such local events is still required, as previous cortisol measurements in the dog were performed at the circulating level [14, 23-25]. Furthermore, as already stated, termination of pregnancy in the dog is associated with increased circulating PGF2α levels, deriving from the trophoblast and involving the 9-keto PGE2 reductase (9KPGR)-mediated synthesis from PGE2 [49]. An interplay between PGF2α and cortisol has been described in several instances [1, 4]. However, the extent to which cortisol directly contributes to the placental PGF2α output affecting the synthetic cascade of prostaglandins in the dog, including the rising COX2/PTGS2 activity [21], remains to be investigated.

5. Conclusions

The results from the present work describe, for the first time, the presence of stage-dependent cortisol-modulating mechanisms in the canine placenta, mainly associated with the trophoblast. The higher expression of HSD11B2 in early placentation, associated with the local tissue potential to inactivate cortisol, might be involved in protective mechanisms of the embryo against maternal-derived glucocorticoids. The P4-dependent regulation of HSD11B2 is further substantiated by observation both during normal and induced parturition/abortion. A clear shift in placental regulation of cortisol activity is apparent at term, with parturition being associated with an increased *HSD11B1* mRNA availability, and decreased HSD11B2 expression and cortisol-inactivating activity. An interplay between different trophoblast populations is also apparent, with HSD11B1 being mainly localized in the cytotrophoblast, where GR/NR3C1 is also expressed [29], while HSD11B2-positive signals were mainly observed in the syncytiotrophoblast. Although its definitive role remains still to be defined for the dog, in accordance with our hypothesis, local cortisol appears to be involved in the termination of canine pregnancy and deserves more attention in the future.

Conflict of interests

The authors declare that they have no conflicts of interest.

Author's contributions

MTP was involved in developing the concept of the present study, experimental design, generating data, analysis and interpretation of data and drafting of the manuscript. GS was involved in the generation, analysis and interpretation of data, and revision of the manuscript. SA, RPC, IMR and KR were involved in the collection of tissue material, knowledge transfer, critical discussion and interpretation of data, and revision of the manuscript. MPK designed and supervised the project, was involved in interpretation of the data, and drafting and revision of the manuscript. All authors read and approved the final manuscript.

Acknowledgements

Authors are thankful to Dr. Sharon Mortimer for the careful editing of the manuscript. The technical expertise and contributions of Ricardo Fernandez Rubia and Kirstin Skaar are greatly appreciated. Part of the laboratory work was performed using the logistics at the Center for Clinical Studies, Vetsuisse Faculty, University of Zurich.

Figure legends

Figure 1. Relative gene expression of HSD11B1 and HSD11B2 in the canine uterus/utero-placental compartment during pregnancy and in response to antigestagens.

Relative gene expression is presented as determined by semi-quantitative real time (TaqMan) PCR ($\bar{X}$ +/- SD). **(A-D)** To evaluate the effects of pregnancy progression, or of preterm termination of pregnancy with aglepristone, one-way non-parametric ANOVA was applied, revealing: **(A)** $P < 0.0001$, **(B)** $P = 0.0197$, **(C)** $P < 0.0001$ and **(D)** $P = 0.0009$. When $P < 0.05$, analysis was followed by a Tukey-Kramer multiple comparison post-test. **(E, F)** Comparison of relative gene expression between *HSD11B1* and *HSD11B2* at each stage was evaluated by applying Student's unpaired two-tailed t- test. Bars with asterisks differ at: * $P < 0.05$, ** $P < 0.01$, *** $P < 0.001$. E- = embryo-negative/non-pregnant animals, E+ = embryo-positive/pre-implantation, day 17 = time of implantation, Post-Imp = post-implantation, Mid-Gest = mid-gestation.

Figure 2. Compartmentalization of HSD11B1 and HSD11B2 relative mRNA levels in the utero-placental tissue during mid-gestation and prepartum luteolysis. Relative gene expression, presented as $\bar{X}$ +/- SD, was determined by semi-quantitative real time (TaqMan) PCR. Samples from 3 animals for each pregnancy stage were used. Differences between all groups was assessed with one-way non-parametric ANOVA, with $P = 0.0079$ for HSD11B1 and $P < 0.0001$ for HSD11B1, followed by a Tukey-Kramer multiple comparison post-test. As the expression of both factors was frequently below detection limits in myometrium during mid-gestation, these samples were removed from statistical analysis. Bars with asterisks differ at: * $P < 0.05$, ** $P < 0.01$, *** $P < 0.001$.

Figure 3. Protein expression of HSD11B2 in utero-placental homogenates. (A) Epitope-blocking peptide was used to block HSD11B2-specific signal (~44kDa) in protein extract of utero-placental homogenates. **(B)** Representative immunoblots for HSD11B2 and ACTINB are shown. Standardized optical density (SOD) of HSD11B2 signals was measured in proteins extracted from utero-placental samples collected during post-implantation (Post-Imp), mid-gestation (Mid-Gest) and prepartum luteolysis. After quantifying HSD11B2 signals, membranes were re-blotted targeting ACTINB for normalization of signals intensity. SOD are presented as $\bar{X}$ +/- SD. One-way non-parametric ANOVA revealed $p = 0.0005$, followed by a Tukey-Kramer multiple comparison post-test.

Figure 4. Immunohistochemical localization of HSD11B2 in the canine placental labyrinth at selected stages of pregnancy. (A) During post-implantation, signals were observed in the invading trophoblast. In the mature mid-gestation placenta, strong positive signals were localized in syncytiotrophoblast cells, with weak signals also being observed in other placental cell populations (e.g. endothelial and decidual cells). Samples collected at the time of prepartum luteolysis appear to present a weaker and more diffuse pattern of staining. **(B)** The localization of HSD11B2-positive signals in the syncytiotrophoblast of the matured placenta was confirmed by performing consecutive staining of mid-gestation samples targeting PGR (expressed by decidual cells) and ETB (expressed by syncytiotrophoblast cells). No staining was observed in the isotype controls (insets in pictures, at the same magnification). Solid arrow = decidual cell; open arrow = endothelial cell; closed arrowhead = cytotrophoblast; open arrowhead = syncytiotrophoblast; asterisk = fetal stroma.

Figure 5. Localization of *HSD11B1* and *HSD11B2* mRNA in the canine placental labyrinth at mid-gestation and prepartum luteolysis. (A) *HSD11B1*-positive signals were mainly localized in cytotrophoblast and endothelial cells. Signal intensity in endothelial cells appeared to be stronger at prepartum luteolysis than at mid-gestation. (B) *HSD11B2* was mainly expressed in the syncytiotrophoblast during mid-gestation, with a more diffuse pattern being observed at the time of prepartum luteolysis. No staining was observed in the negative controls (sense probe; insets in pictures, at the same magnification). Open arrow = endothelial cell; closed arrowhead = cytotrophoblast; open arrowhead = syncytiotrophoblast.

Figure 6. Interconversion rate between cortisol and cortisone performed by canine utero-placental microsomes isolated from different stages of pregnancy. Microsome conversion rates of cortisol into cortisone are presented as a percentage. Differences between groups was assessed with one-way non-parametric ANOVA ($P = 0.0186$), followed by a Tukey-Kramer multiple comparison post-test. Bars with asterisks differ at: * $P < 0.05$.

5. References

1. Whittle, W.L., et al., *Glucocorticoid regulation of human and ovine parturition: the relationship between fetal hypothalamic-pituitary-adrenal axis activation and intrauterine prostaglandin production.* Biol Reprod, 2001. **64**(4): p. 1019-32.
2. Cottrell, E.C. and J.R. Seckl, *Prenatal stress, glucocorticoids and the programming of adult disease.* Front Behav Neurosci, 2009. **3**: p. 19.
3. Liggins, G.C., et al., *The mechanism of initiation of parturition in the ewe.* Recent Prog Horm Res, 1973. **29**: p. 111-59.
4. Schuler, G., R. Fürbass, and K. Klisch, *Placental contribution to the endocrinology of gestation and parturition.* Animal Reproduction, 2018. **15**(Suppl. 1): p. 822-842.

5. Tulchinsky, D., et al., *Plasma estrone, estradiol, estriol, progesterone, and 17-hydroxyprogesterone in human pregnancy. I. Normal pregnancy.* Am J Obstet Gynecol, 1972. **112**(8): p. 1095-100.
6. Heap, R.B. and R. Deanesly, *Progesterone in systemic blood and placentae of intact and ovariectomized pregnant guinea-pigs.* J Endocrinol, 1966. **34**(4): p. 417-23.
7. Mitchell, B.F. and M.J. Taggart, *Are animal models relevant to key aspects of human parturition?* Am J Physiol Regul Integr Comp Physiol, 2009. **297**(3): p. R525-45.
8. Nnamani, M.C., et al., *Evidence for independent evolution of functional progesterone withdrawal in primates and guinea pigs.* Evol Med Public Health, 2013. **2013**(1): p. 273-88.
9. Zakar, T. and F. Hertelendy, *Progesterone withdrawal: key to parturition.* Am J Obstet Gynecol, 2007. **196**(4): p. 289-96.
10. Ojasoo, T., et al., *Binding of steroids to the progestin and glucocorticoid receptors analyzed by correspondence analysis.* J Med Chem, 1988. **31**(6): p. 1160-9.
11. Philibert, D., et al., *From RU 38486 towards Dissociated Antiglucocorticoid and Antiprogesterone.* Frontiers of Hormone Research, 1991. **19**: p. 1-17.
12. Karalis, K., G. Goodwin, and J.A. Majzoub, *Cortisol blockade of progesterone: a possible molecular mechanism involved in the initiation of human labor.* Nat Med, 1996. **2**(5): p. 556-60.
13. Ogle, T.F. and B.K. Beyer, *Steroid-binding specificity of the progesterone receptor from rat placenta.* J Steroid Biochem, 1982. **16**(2): p. 147-50.
14. Hoffmann, B., et al., *Investigations on hormonal changes around parturition in the dog and the occurrence of pregnancy-specific non conjugated oestrogens.* Exp Clin Endocrinol, 1994. **102**(3): p. 185-189.
15. Nishiyama, T., et al., *Immunohistochemical study of steroidogenic enzymes in the ovary and placenta during pregnancy in the dog.* Anat Hist Embryol, 1999. **28**(2): p. 125-129.
16. Onclin, K., B. Murphy, and J.P. Verstegen, *Comparisons of estradiol, LH and FSH patterns in pregnant and nonpregnant beagle bitches.* Theriogenology, 2002. **57**(8): p. 1957-1972.
17. Kowalewski, M.P., et al., *The Dog: Nonconformist, Not Only in Maternal Recognition Signaling.* Adv Anat Embryol Cell Biol, 2015. **216**: p. 215-37.
18. Kowalewski, M.P., *Selected comparative aspects of canine female reproductive physiology*, in *Encyclopedia of Reproduction*, M.K. Skinner, Editor. 2018, Academic Press. p. 682-691.
19. Vermeirsch, H., P. Simoens, and H. Lauwers, *Immunohistochemical detection of the estrogen receptor-α and progesterone receptor in the canine pregnant uterus and placental labyrinth.* The Anatomical Record, 2000. **26**.
20. Kowalewski, M.P., et al., *Canine Endotheliochorial Placenta: Morpho-Functional Aspects.* Adv Anat Embryol Cell Biol, 2021. **234**: p. 155-179.
21. Kowalewski, M.P., et al., *Canine placenta: a source of prepartal prostaglandins during normal and antiprogestin-induced parturition.* Reproduction, 2010. **139**(3): p. 655-64.
22. Kowalewski, M.P., M. Tavares Pereira, and A. Kazemian, *Canine conceptus-maternal communication during maintenance and termination of pregnancy, including the role of species-specific decidualization.* Theriogenology, 2020. **150**: p. 329-338.
23. Concannon, P.W., et al., *Parturition and Lactation in the Bitch: Serum Progesterone, Cortisol and Prolactin.* Biology of Reproduction, 1978. **19**(5).
24. Veronesi, M.C., et al., *Correlations among body temperature, plasma progesterone, cortisol and prostaglandin F2alpha of the periparturient bitch.* J Vet Med A Physiol Pathol Clin Med, 2002. **49**(5): p. 264-8.
25. Olsson, K., et al., *Increased plasma concentrations of vasopressin, oxytocin, cortisol and the prostaglandin F2alpha metabolite during labour in the dog.* Acta Physiol Scand, 2003. **179**(3): p. 281-7.
26. Zone, M., et al., *Termination of pregnancy in dogs by oral administration of dexamethasone.* Theriogenology, 1995. **43**(2): p. 487-494.
27. Wanke, M., et al., *Clinical use of dexamethasone for termination of unwanted pregnancy in dogs.* J Reprod Fertil Suppl, 1997. **51**: p. 233-8.
28. Austad, R., A. Lunde, and O.V. Sjaastad, *Peripheral plasma levels of oestradiol-17 beta and progesterone in the bitch during the oestrous cycle, in normal pregnancy and after dexamethasone treatment.* J Reprod Fertil, 1976. **46**(1): p. 129-36.
29. Gram, A., et al., *Elevated utero/placental GR/NR3C1 is not required for the induction of parturition in the dog.* Reproduction, 2016. **152**(4): p. 303-11.
30. Nowak, M., et al., *Gene expression profiling of the canine placenta during normal and antigestagen-induced luteolysis.* Gen Comp Endocrinol, 2019. **282**: p. 113194.
31. Chapman, K., M. Holmes, and J. Seckl, *11beta-hydroxysteroid dehydrogenases: intracellular gate-keepers of tissue glucocorticoid action.* Physiol Rev, 2013. **93**(3): p. 1139-206.
32. Seckl, J.R. and B.R. Walker, *Minireview: 11beta-hydroxysteroid dehydrogenase type 1- a tissue-specific amplifier of glucocorticoid action.* Endocrinology, 2001. **142**(4): p. 1371-6.
33. Seckl, J.R. and M.J. Meaney, *Glucocorticoid programming.* Ann N Y Acad Sci, 2004. **1032**: p. 63-84.
34. Kowalewski, M.P., et al., *Luteal and placental function in the bitch: spatio-temporal changes in prolactin receptor (PRLr) expression at dioestrus, pregnancy and normal and induced parturition.* Reproductive Biology and Endocrinology, 2011. **9**(109).
35. Gram, A., A. Boos, and M.P. Kowalewski, *Uterine and placental expression of canine oxytocin receptor during pregnancy and normal and induced parturition.* Reprod Domest Anim, 2014. **49 Suppl 2**: p. 41-9.

36. Kowalewski, M.P., et al., *Time related changes in luteal prostaglandin synthesis and steroidogenic capacity during pregnancy, normal and antiprogestin induced luteolysis in the bitch.* Anim Reprod Sci, 2009. **116**(1-2): p. 129-38.
37. Graubner, F.R., et al., *Decidualization of the canine uterus: From early until late gestational in vivo morphological observations, and functional characterization of immortalized canine uterine stromal cell lines.* Reprod Domest Anim, 2017. **52 Suppl 2**: p. 137-147.
38. Concannon, P.W., J.P. McCann, and M. Temple, *Biology and endocrinology of ovulation, pregnancy and parturition in the dog.* J Reprod Fertil Suppl, 1989. **39**(0449-3087): p. 3-25.
39. Amoroso, E.C., *Placentation*, in *Marshall's Physiology of Reproduction*, A.S. Parkes, Editor. 1952, Longmans, Greens and Co: London, UK.
40. Tavares Pereira, M., et al., *Prostaglandin-mediated effects in early canine corpus luteum: in vivo effects on vascular and immune factors.* Reprod Biol, 2019. **19**(1): p. 100-111.
41. Kowalewski, M.P., et al., *Expression of cyclooxygenase 1 and 2 in the canine corpus luteum during diestrus.* Theriogenology, 2006. **66**(6-7): p. 1423-30.
42. Nowak, M., S. Aslan, and M.P. Kowalewski, *Determination of novel reference genes for improving gene expression data normalization in selected canine reproductive tissues - a multistudy analysis.* BMC Vet Res, 2020. **16**(1): p. 440.
43. Xie, F., et al., *miRDeepFinder: a miRNA analysis tool for deep sequencing of plant small RNAs.* Plant Molecular Biology, 2012. **80**(1): p. 75-84.
44. Nowak, M., et al., *Functional implications of the utero-placental relaxin (RLN) system in the dog throughout pregnancy and at term.* Reproduction, 2017. **154**(4): p. 415-431.
45. Gram, A., A. Boos, and M.P. Kowalewski, *Cellular localization, expression and functional implications of the utero-placental endothelin system during maintenance and termination of canine gestation.* 2017.
46. Kowalewski, M.P., et al., *Characterization of the canine 3beta-hydroxysteroid dehydrogenase and its expression in the corpus luteum during diestrus.* J Steroid Biochem Mol Biol, 2006. **101**(4-5): p. 254-62.
47. Tavares Pereira, M., et al., *Luteal expression of factors involved in the metabolism and sensitivity to oestrogens in the dog during pregnancy and in non-pregnant cycle.* Reprod Domest Anim, 2021.
48. Gram, A., et al., *Biosynthesis and degradation of canine placental prostaglandins: prepartum changes in expression and function of prostaglandin F2alpha-synthase (PGFS, AKR1C3) and 15-hydroxyprostaglandin dehydrogenase (HPGD).* Biol Reprod, 2013. **89**(1): p. 2.
49. Gram, A., et al., *Canine placental prostaglandin E2 synthase: expression, localization, and biological functions in providing substrates for prepartum PGF2alpha synthesis.* Biol Reprod, 2014. **91**(6): p. 154.
50. Li, X., et al., *Effects of Ziram on Rat and Human 11beta-Hydroxysteroid Dehydrogenase Isoforms.* Chem Res Toxicol, 2016. **29**(3): p. 398-405.
51. Turpeinen, U., et al., *Determination of urinary free cortisol by HPLC.* Clin Chem, 1997. **43**(8 Pt 1): p. 1386-91.
52. Jafari, Z., et al., *The Adverse Effects of Auditory Stress on Mouse Uterus Receptivity and Behaviour.* Sci Rep, 2017. **7**(1): p. 4720.
53. Li, Q.N., et al., *Glucocorticoid exposure affects female fertility by exerting its effect on the uterus but not on the oocyte: lessons from a hypercortisolism mouse model.* Hum Reprod, 2018. **33**(12): p. 2285-2294.
54. Rogers, S.L., et al., *Diminished 11beta-hydroxysteroid dehydrogenase type 2 activity is associated with decreased weight and weight gain across the first year of life.* J Clin Endocrinol Metab, 2014. **99**(5): p. E821-31.
55. Belkacemi, L., et al., *Altered placental development in undernourished rats: role of maternal glucocorticoids.* Reprod Biol Endocrinol, 2011. **9**: p. 105.
56. Togher, K.L., et al., *Epigenetic regulation of the placental HSD11B2 barrier and its role as a critical regulator of fetal development.* Epigenetics, 2014. **9**(6): p. 816-22.
57. Zheng, H.T., et al., *Progesterone-regulated Hsd11b2 as a barrier to balance mouse uterine corticosterone.* J Endocrinol, 2020. **244**(1): p. 177-187.
58. Zhu, P., et al., *Mechanisms for establishment of the placental glucocorticoid barrier, a guard for life.* Cell Mol Life Sci, 2019. **76**(1): p. 13-26.
59. Beitins, I.Z., et al., *The Metabolic Clearance Rate, Blood Production, Interconversion and Transplacental Passage of Cortisol and Cortisone in Pregnancy Near Term.* Pediatric Research, 1973. **7**(5): p. 509-519.
60. Fusi, J., et al., *The usefulness of claws collected without invasiveness for cortisol and dehydroepiandrosterone (sulfate) monitoring in healthy newborn puppies after birth.* Theriogenology, 2018. **122**: p. 137-143.
61. Groppetti, D., et al., *Maternal and neonatal canine cortisol measurement in multiple matrices during the perinatal period: A pilot study.* PLoS One, 2021. **16**(7): p. e0254842.
62. Thompson, A., V.K. Han, and K. Yang, *Spatial and temporal patterns of expression of 11beta-hydroxysteroid dehydrogenase types 1 and 2 messenger RNA and glucocorticoid receptor protein in the murine placenta and uterus during late pregnancy.* Biol Reprod, 2002. **67**(6): p. 1708-18.
63. Krozowski, Z., et al., *Immunohistochemical localization of the 11 beta-hydroxysteroid dehydrogenase type II enzyme in human kidney and placenta.* J Clin Endocrinol Metab, 1995. **80**(7): p. 2203-9.
64. Simmons, R.M., et al., *HSD11B1, HSD11B2, PTGS2, and NR3C1 expression in the peri-implantation ovine uterus: effects of pregnancy, progesterone, and interferon tau.* Biol Reprod, 2010. **82**(1): p. 35-43.
65. Kowalewski, M.P., *Luteal regression vs. prepartum luteolysis: regulatory mechanisms governing canine corpus luteum function.* Reprod Biol, 2014. **14**(2): p. 89-102.
66. Kowalewski, M.P., et al., *Progesterone receptor blockers: historical perspective, mode of function and insights into clinical and scientific applications.* Tierarztl Prax Ausg K Kleintiere Heimtiere, 2020. **48**(6): p. 433-440.

67. Sun, K., K. Yang, and J.R. Challis, *Differential expression of 11 beta-hydroxysteroid dehydrogenase types 1 and 2 in human placenta and fetal membranes.* J Clin Endocrinol Metab, 1997. **82**(1): p. 300-5.
68. Bolt, R.J., et al., *Glucocorticoids and lung development in the fetus and preterm infant.* Pediatr Pulmonol, 2001. **32**(1): p. 76-91.

Utero-placental expression and functional implications of HSD11B1 and HSD11B2 in canine pregnancy

Miguel Tavares Pereira[1]; Gerhard Schuler[2]; Selim Aslan[3]; Rita Payan-Carreira[4]; Iris M Reichler[5]; Karine Reynaud[6,7]; Mariusz P Kowalewski[1,8]

[1]Institute of Veterinary Anatomy, Vetsuisse Faculty, University of Zurich (UZH), Zurich, Switzerland
[2]Clinic for Obstetrics, Gynecology and Andrology of Large and Small Animals, Justus-Liebig-University, Giessen, Germany
[3]Department of Obstetrics and Gynecology, Faculty of Veterinary Medicine, Near East University, Nicosia, Cyprus
[4]School of Science and Technology, Department of Veterinary Medicine, University of Évora, Évora, Portugal
[5]Clinic for Reproductive Medicine, Vetsuisse Faculty, University of Zurich (UZH), Zurich, Switzerland
[6]École Nationale Vétérinaire d'Alfort, EnvA, 94700 Maisons-Alfort, France
[7]Physiologie de la Reproduction et des Comportements, CNRS, IFCE, INRAE, Université de Tours, PRC, Nouzilly, France
[8]Center for Clinical Studies (ZKS), Vetsuisse Faculty, University of Zurich (UZH), Zurich, Switzerland

Grant Support

The present work was supported by the Swiss National Science Foundation (SNSF) research grant number 31003A_182481.

Correspondence:
Prof. Dr. Mariusz P. Kowalewski, PhD
Institute of Veterinary Anatomy
Vetsuisse Faculty
University of Zurich
Winterthurerstrasse 260
CH-8057 Zurich, Switzerland
Tel.: 0041-44-6358784; Fax.: 0041-44-6358943
Email: kowalewskipl@yahoo.de or kowalewski@vetanat.uzh.ch

Email addresses:
MTP: miguel.tavarespereira@uzh.ch
GS: Gerhard.Schuler@vetmed.uni-giessen.de
RPC: rtpayan@uevora.pt
SA: selim.aslan@neu.edu.tr
IMR: ireichler@vetclinics.uzh.ch
KR: karine.reynaud@inrae.fr
MPK: kowalewski@vetanat.uzh.ch or kowalewskipl@yahoo.de

Running title

HSD11B1 and -2 expression in the canine placenta

Summary Sentence

The canine placenta appears to have increased trophoblast-mediated inactivation of cortisol during mid-pregnancy, whereas parturition appears to be marked by increased local cortisol availability.

Keywords
dog (*Canis lupus familiaris*), placenta, parturition, cortisol, hydroxysteroid 11-beta dehydrogenase (HSD11B) 1/2

Abstract

Apart from being stress mediators, glucocorticoids modulate the feto-maternal interface during the induction of parturition. In the dog, the prepartum rise of cortisol in the maternal circulation appears to be erratic, and information about its contribution to the prepartum luteolytic cascade is scarce. However, the local placental upregulation of glucocorticoid receptor (GR/NR3C1) at term led to the hypothesis that species-specific regulatory mechanisms might apply to the involvement of cortisol in canine parturition. Therefore, here, we assessed the canine uterine/utero-placental spatio-temporal expression of hydroxysteroid 11-beta dehydrogenase 1 (HSD11B1; reduces cortisone to cortisol), and -2 (HSD11B2; oxidizes cortisol to the inactive cortisone). Both enzymes were detectable throughout pregnancy, their transcriptional levels were elevated following implantation, with a strong increase in *HSD11B2* post-implantation (days 18-25 of pregnancy), and in *HSD11B1* at mid-gestation (days 35-40) (P<0.05).". Interestingly, when compared pairwise, *HSD11B2* transcripts were higher during post-implantation, whereas *HSD11B1* dominated during mid-gestation and luteolysis (P<0.05). A custom-made species-specific antibody generated against HSD11B2 confirmed its decreased expression at prepartum luteolysis. Moreover, in mid-pregnant dogs treated with aglepristone, *HSD11B1* was significantly higher than *-2* (P<0.05). HSD11B2 (protein and transcript) was localized mostly in the syncytiotrophoblast, whereas *HSD11B1* mRNA was mainly localized in cytotrophoblast cells. Finally, in a functional approach using placental microsomes, a reduced conversion capacity to deactivate cortisol into cortisone was observed during prepartum luteolysis, fitting well with the diminished HSD11B2 levels. In particular, the latter findings support the presence of local increased cortisol availability at term in the dog, contrasting with an enhanced inactivation of cortisol during early pregnancy.

1. Introduction

The adrenal-derived cortisol, besides its association with stress, is involved in biological processes including reproductive events such as fetal development and the parturition cascade [1, 2]. Parturition is an orchestrated, mostly species-specific event, involving complex

endocrine signaling cascades that are still not fully characterized in several eutherian species. The sheep is one of the animal species in which the initiation of parturition is well studied and serves as a translational model for other domestic animal species. Thus, in this animal model, parturition appears to be triggered by increased amounts of fetal adrenal-derived cortisol [1, 3], inducing a shift in placental steroidogenic activity towards increased estradiol (E2) production, replacing the local progesterone (P4) production. This leads to increased secretion of placental prostaglandin (PG) F2α, which stimulates myometrial activity [1, 3]. The luteolytic activity of cortisol-induced and placenta-derived PGF2α plays further important roles in species where the corpus luteum is, at least in part, the source of P4, e.g., pig, cow, goat, mouse, cat, and rabbit [4]. Interestingly, in guinea pigs, humans, and other primates, parturition occurs in the presence of high circulating amounts of P4, accompanied, however, by local, i.e., placental, withdrawal of P4 signaling [5-8]. Accordingly, several mechanisms, involving local metabolism, differential expression of P4 receptor (PGR) isoforms, synthesis and availability of lower activity P4 metabolites, and accessibility of transcription factors, have been implied in the underlying regulatory mechanisms [s. reviewed in 7, 9]. In addition, the competitive binding activity observed between the glucocorticoid receptor (GR/NR3C1) and PGR [10, 11] is also thought to contribute to the functional local withdrawal of P4 in human placenta [12]. In contrast, cortisol appears to have a low binding capacity to PGR at physiological levels [10, 13].

The unique endocrinological features of the dog, when compared with other domestic mammals, hinder the translation of different parturition-associated biological strategies observed in other species. The dog is the only domestic mammal in which no steroidogenic activity is observed in the placenta, with P4 being produced solely by the corpus luteum (CL) [14, 15]. This further accounts for the absence of a parturition-specific increase of estrogens [14, 16]. Furthermore, due to the absence of anti-luteolytic mechanisms during early diestrus, the dog presents an inherently regulated and long lasting activity of the CL [17, 18]. In the canine endotheliochorial placenta, maternal stroma-derived decidual cells are the only cellular population expressing the nuclear PGR [19-21]. This distribution of PGR is especially important when considering the parturition cascade. The prepartum decline of circulating P4 levels, or functional blocking of PGR with antigestagens (e.g., aglepristone), results in decreased decidual cell-mediated P4/PGR signaling, associated with increased prepartum production of luteolytic PGF2α by the trophoblast, and leading to parturition/abortion [22].

Regarding canine cortisol, increased circulating amounts have been reported in dogs at the time of parturition [14, 23-25]. However, due to wide variation in detected levels, ranging from nadir

to clearly measurable values, elevated circulating cortisol levels are not considered a prerequisite for the induction of parturition in dogs and could be indicative of maternal stress [14, 23]. Nevertheless, despite its weak clinical applicability (repeated treatments with high dosages over longer time, associated with strong side effects), the termination of canine pregnancy can be induced with exogenously-administered glucocorticoids during the last third of pregnancy [26-28]. Furthermore, GR/NR3C1 was detected in the canine fetal trophoblast, and was upregulated in the placenta at the time of prepartum luteolysis [29]. Interestingly, in samples collected after preterm induction of luteolysis with aglepristone, GR/NR3C1 expression remained unaffected, despite the increased PGF2α output observed following treatment [21]. Jointly, these observations exclude the increased availability of GR/NR3C1 as a requirement for the prepartum release of PGF2α in the dog [29]. Instead, it was proposed that GR/NR3C1 could be involved in a P4 withdrawal mechanism [29], similar to its proposed role in humans [12].

Underlying the present project, we hypothesized that glucocorticoids might be involved in the parturition cascade in the dog, and that their signaling and availability might be regulated locally in the placenta. Accordingly, recently, changes in the placental transcriptional profile during parturition were investigated in canine placental samples collected during mid-pregnancy and at the time of luteolysis, both prepartum and antigestagen-induced (abortion at mid-term) [30]. Among the differentially expressed genes were factors identified as potentially modulated by P4, i.a., hydroxysteroid 11-beta dehydrogenase 2 (*HSD11B2*), that, although being initially abundantly expressed, was downregulated during the termination of pregnancy [30]. HSD11B2, together with HSD11B1, interconvert the biologically inactive cortisone and the active cortisol [31]. HSD11B1 is predominantly a reductase, reducing cortisone into cortisol, and is expressed in several tissues (e.g., liver, adipose tissue and placenta, central nervous system, cardiovascular system or immune system), where it increases the intracellular glucocorticoid availability [31, 32]. Moreover, HSD11B1 can act as a dehydrogenase under specific circumstances, mainly associated with the disruption of cellular activity and/or metabolic disturbances like diabetes or obesity [31, 32]. In contrast, HSD11B2 acts solely as a dehydrogenase, decreasing local cortisol availability by converting it into cortisone [31]. The cortisol-inactivating function of HSD11B2 in the placenta acts as a protective mechanism against the passage of glucocorticoids into fetal circulation in humans [33]. However, the only information to date about these factors in the canine placenta is from the transcriptomic study [30]. To contribute to the knowledge regarding local regulatory mechanisms, and test our hypothesis regarding the local involvement of cortisol metabolism in the maintenance of canine

pregnancy, we investigated the expression and regulation of HSD11B1 and -2 in the canine uterus and/or placenta throughout pregnancy.

2. Materials and Methods

2.1 Tissue collection and preservation

Uterine/utero-placental samples from 41 clinically healthy crossbred sexually mature bitches were collected by routine ovariohysterectomy. Several of these tissue samples originated from previous studies, where details on animal manipulation and staging of pregnancy are described [21, 30, 34-37]. Animal experiments were carried out in accordance with animal welfare ethical principles and legislation, and approved by the responsible ethics committees of the Justus-Liebig University Giessen, Germany (permits no. II 25.3-19c20- 15c GI 18/14 and VIG3-19c-20/ 15 GI 18,14); of the University of Ankara, Turkey (permits no. Ankara 2006/06 and 2008–25– 124); and of the national review board CNREEA #16 (APAFIS #2015042112442132) for the Alfort Veterinary School (facility 947-046-2), France. Further samples from animals submitted to routine ovariohysterectomy at the Section of Small Animal Reproduction, Vetsuisse Faculty, Zurich, were collected after the owners' informed consent.

The onset of spontaneous estrus was observed in all animals, with the day of ovulation being determined when circulating P4 concentration exceeded 5 ng/ml. After the required period for oocyte maturation in the oviduct, i.e., 2-3 days [17], animals were mated (day 0 of pregnancy). Uterine or utero-placental samples (depending on the pregnancy stage) were divided in the following groups: non-pregnant animals (E-, days 8 - 12 after mating, n = 5), pre-implantation (E+, days 8 - 12 of pregnancy, n = 5), time of implantation (Day 17, n = 4), post-implantation (Post-Imp, days 18 – 25 of pregnancy, n = 7), mid-gestation (Mid-Gest, days 35 - 40 of pregnancy, n = 6), prepartum luteolysis (Lut, n = 4), 24h after aglepristone treatment (Agle 24h, n = 5) and 72h after aglepristone treatment (Agle 72h, n = 5). As implantation takes place at day 17 [20, 38, 39], confirmation of pregnancy during early pre-implantation period was performed with embryo flushing (E+). Animals in which no embryos could be retrieved between days 8 - 12 were allocated to the non-pregnant control group (E-). Samples from the Lut group were collected during active prepartum P4 decline, determined by hormonal measurements every 6h until P4 concentrations were below 3 ng/ml in three consecutive assessments. Aglepristone (Alizine, Virbac, Bad Oldesloe, Germany) was used to induce the termination of pregnancy in 10 animals at mid-pregnancy (days 40 – 45 after mating), following the protocol provided by the supplier, i.e., administration of 10 mg/kg body weight twice 24h

apart. Samples containing uterine and placental sections were collected 24 or 72h after the second administration of aglepristone.

After surgery, samples were washed with PBS and dissected from connective tissue. Samples used for RNA and protein analysis were immersed in RNAlater (Ambion Biotechnology GmbH, Wiesbaden, Germany) at 4ºC for 24h and then stored at -80ºC until needed. For histology, samples were fixed in 10% phosphate-buffered formalin for 24h, washed with PBS for 7 consecutive days, dehydrated in an ethanol series, transferred into xylol and embedded in paraffin. Whereas all samples were used for TaqMan PCR, 3 samples/group were used for immunohistochemistry and *in situ* hybridization experiments.

2.2 RNA isolation, reverse transcription and semi-quantitative real-time TaqMan PCR

The isolation of total RNA was performed with TRIzol reagent (Invitrogen, Varlsbad, CA, USA), following the supplier's instructions. A NanoDrop 2000 spectrophotometer (ThermoFisher Scientific AG, Reinach, Switzerland) was used to assess RNA quantity and purity. For each sample, RNA was cleaned of possible contaminating genomic DNA with the RQ1 RNA-free DNase kit (Promega, Dübendorf, Switzerland), and reverse transcribed using the MultiScribe Reverse Transcriptase with random hexamers used as primers (Applied Biosystems by Thermo Fisher, Foster City, CA, USA); cDNA corresponding to 1.2µg of total RNA was used per sample and reaction. The relative gene expression was assessed by semi-quantitative real time TaqMan PCR, following the previously described protocol [40, 41], in an ABI PRISM 7500 Sequence Detection System fluorometer (Applied Biosystems). All reactions were run in duplicate with Fast Start Universal Probe Master (Roche Diagnostics AG, Basel, Switzerland) and gene expression TaqMan assays targeting *HSD11B1* (Cf02626817_m1) and *HSD11B2* (Cf02690463_s1), all obtained from Applied Biosystems. Autoclaved water and non-reverse transcribed DNase-treated RNA were used as negative controls. Relative quantification was performed with the comparative Ct method (ΔΔCt), following logarithmic transformation of values, calibrated to the average expression among all samples, and normalized to the expression of reference genes. Initially, three reference genes were evaluated, following our recent description [42]: *PTK2* (Cf02684608_m1), *EIF4H* (Cf02713640_m1) and *KDM4A* (Cf02708629_m1). The evaluation of the stability of the reference genes was further assessed with RefFinder [43]. Since PTK2 and KDM4A were more stable than EIF4H in the samples used in this study, these two genes were used for the ΔΔCt calculation.

For the compartmentalization studies, formalin-fixed and paraffin-embedded (FFPE) utero-placental samples from 3 animals belonging to Mid-Gest or Lut groups were used, according to our previously described protocol [29, 44]. A total of 3 tissue sections per animal were cut with 5 μm thickness and mounted on Arcturus PEN membrane glass slides (LCM0522, Applied Biosystems). Tissue sections were then deparaffinized, rehydrated, stained with hematoxylin for histological visualization and dried overnight at 37ºC. Using a stereomicroscope, the different utero-placental compartments (i.e., placental labyrinth, endometrium and myometrium) were identified and dissected with sterile scalpel blades. Total RNA was isolated using the RNeasy FFPE Kit (Qiagen GmBH, Hilden, Germany), following the manufacturer's protocol, and RNA concentration was measured with a NanoDrop 2000. Following the variable, and sometimes low, yield of RNA obtained from these samples (ranging 43 to 416 ng/μl), 10 ng of RNA were DNase treated and reverse transcribed with the High Capacity cDNA Reverse Transcription Kit (Applied Biosystems). Afterwards, the obtained cDNA was amplified with the TaqMan PreAmp Master Mix kit, following the supplier's protocols and as previously described [40]. For this, TaqMan assays for *HSD11B1*, *HSD11B2* and reference genes were pooled and mixed with the previously prepared cDNA and TaqMan Preamp Master Mix. Samples were then amplified using an Eppendorf Mastercycler (Vaudax-Eppendorf AG, Basel, Switzerland). Following this, the semi-quantitative PCR and relative gene expression quantification was performed as described above.

2.3 Immunohistochemistry (IHC)

Since no species-specific or cross-reacting antibodies were commercially available for the canine species, the development of polyclonal antibodies was attempted, as previously described [44], and was successful for generating a custom-made anti-HSD11B2 antibody (but not for HSD11B1) (Eurogentec Seraing, Belgium). Therefore, guinea pigs were immunized using the peptide sequence C+RALRPGQPGSTPAQ (aa 270-284) and C+LAAQPRRRYYPGRGL (aa226-240), based on the available sequences (GenBank accession number XM_005620822.3). Cysteine (C+) was added to the N-terminal to allow peptide conjugation to carrier proteins, and the NH2-terminus was added to the C-end of the peptide to mimic the uncharged peptide bond in the protein. After preliminary assessments of IHC staining, the affinity purified antibody targeting the sequence C+RALRPGQPGSTPAQ was used in further analyses.

The standard indirect immunoperoxidase method was used for IHC to localize the expression of HSD11B2 protein in the canine placenta during post-implantation, mid-gestation and

prepartum luteolysis. Additionally, to allow for better differentiation between cell types, consecutively cut slides from mid-gestation animals were stained against the endothelin receptor B (goat polyclonal anti-EDNRB, sc-21196, Santa Cruz Biotechnology), staining for syncytiotrophoblast [45], and nuclear progesterone receptor (mouse monoclonal anti-PGR, IM1408, Beckman Coulter Life Sciences, Indianapolis, IN, USA), staining for decidual cells [21]. IHC was performed as previously described [40, 41]. Sections with 3 µm of FFPE tissue samples were mounted on microscope slides (SuperFrost; Menzel-Glaeser, Braunschweig, Germany), deparaffinized and rehydrated. Antigen retrieval was performed by heating in a microwave oven with Tris-EDTA buffer (10mM Tris base + 1mM EDTA solution, pH = 9, for HSD11B2) or 10mM citrate buffer (pH = 6, for PGR and EDNRB). After quenching endogenous peroxidase activity with 0.3% hydrogen peroxidase in methanol, slides were incubated in 10% goat or horse serum (depending on the secondary antibody) to decrease nonspecific binding, and then incubated overnight at 4ºC with primary antibodies at the following dilutions: anti-HSD11B2 diluted at 1:1000; anti-PGR at 1:100.; EDNRB at 1:200. Pre-immune serum (in the case of HSD11B2) or non-immune IgG (in the case of PGR and EDNRB) were used as negative/isotype controls (goat IgG I-5000, and mouse IgG I-2000, both from Vector Laboratories Inc., Burlingame, CA, USA), at the same protein concentration as the primary antibodies. Following the incubation with a biotinylated secondary antibody diluted at 1:100 (BA-7000 goat anti-guinea pig for HSD11B2; BA-9500 horse anti-goat IgG for EDNRB; BA-2000 horse anti-mouse IgG for PGR; all from Vector Laboratories Inc.) and with streptavidin-peroxidase ABC kit (Vector Laboratories Inc.), positive signals were revealed with the Liquid DAB+ substrate kit (Dako Schweiz AG, Baar, Switzerland). Slides were then counterstained with haematoxylin, dehydrated and mounted with Histokit (Assistant, Osterode, Germany). The localization of positive signals and capture of representative pictures were performed with a Leica DMRXE light microscope equipped with a Leica Flexacam C1 camera (Leica Microsystems, Wetzlar, Germany).

2.4 *In situ* hybridization (ISH)

As the coding sequence available for canine *HSD11B2* in GenBank was only predicted, molecular cloning was performed to confirm the sequence and generate templates for cRNA to be used in ISH. Therefore, the following primers were used: forward: 5'-CCA AGA AGC TAG ATG CCA TG-3', reverse: 5'-CCT GTG GGC ACT GCT CAT T-3' (ordered from Microsynth AG, Balgach, Switzerland), generating amplicons of 937 bp. Hot start PCR was applied with AmpliTaq Gold DNA polymerase (Applied Biosystems) using two uterine cDNA samples;

annealing temperature was set at 58ºC. PCR products were separated on a 2% agarose gel stained with ethidium bromide and isolated using the QIAquick Gel Extraction Kit (Qiagen GmBH). The products were then subcloned into pGEM-T vector (Promega) before transforming into XL1 Blue competent cells (Stratagene, La Jolla, CA, USA) for multiplication. Plasmids were isolated with the PureYield Plasmid Miniprep System (Promega), and control double-digestion was performed with NcoI and NotI restriction enzymes (New England Biolabs, Frankfurt, Germany). Plasmids were then sent for commercial sequencing (Microsynth AG). The partial sequence of canine-specific *HSD11B2* was submitted to GenBank with the accession number.

In the next step, the cellular localization of transcripts encoding for both enzymes was assessed with non-radioactive ISH, following our previously published protocols [21, 46, 47]. Placentae collected during mid-gestation and prepartum luteolysis were used. In addition to the cloned sequence of *HSD11B2* that was used as a template for generating riboprobes, the canine-specific *HSD11B1* sequence was available in GenBank: NM_001005756.1. The following primers were then used for both targets; *HSD11B1* for: 5'-GCA GAA GCA TGG AAG TCA AC-3', rev: 5'-TGA GGC CGA GGA TAC AGA G-3', 251 bp; and *HSD11B2* for: 5'- ACC TCA GCC CAG TCG TAG AT-3', rev: 5'- AGG GCC TTC ATT TGG ATC TGG -3', 248bp (ordered from Microsynth). The PCR products were then purified and subcloned into pGEM-T plasmids following the protocol described above. The specificity and identification of sense and anti-sense direction of products in the plasmid was performed by commercial sequencing of plasmids single cut with either NcoI or NotI restriction enzymes (Microsynth AG), and cRNA probes labelled with digoxigenin (DIG) were synthetized using the DIG-RNA Labelling Kit (Roche Diagnostics AG). The efficiency of riboprobes synthesis was confirmed with a dot-blot analysis, evaluating signal intensity in serial dilutions of the probes in positively charged nylon membranes stained against DIG (Roche Diagnostics AG). In the next step, tissue sections of 2 µm thickness were mounted on microscope slides, deparaffinized in xylene, rehydrated, digested with 70 µg/ml proteinase K for 19 mins at 37ºC (Sigma-Aldrich Chemie GmbH) and post-fixed with 4% paraformaldehyde. *In situ* hybridization of cRNA probes was performed overnight at 37ºC in the presence of formamide. Sense probes served as negative controls. After blocking of nonspecific signals with 3% ovine serum, samples were incubated overnight with alkaline phosphatase-conjugated sheep anti-DIG Fab Fragments diluted 1:5000 (Roche Diagnostics AG). Endogenous alkaline phosphatase signals were blocked with levamisole. Detection of positive signals was performed with 5-bromo-4-chloro-3-indolyl phosphate and nitroblue tetrazolium (BCIP/NBT, Roche Diagnostics AG). Representative pictures were

obtained with a Leica DMRXE light microscope equipped with a Leica Flexacam C1 camera (Leica Microsystems).

2.5 Protein extraction and western blot

The relative protein expression of HSD11B2 was assessed, following our previously published protocols [35, 48]. Randomly selected utero-placental samples from post-implantation, mid-gestation and prepartum luteolysis groups (n = 3/group) were homogenized in lysis buffer (Net2 Buffer: 50 mM Tris–HCl, pH = 7.4, 300 mM NaCl, 0.05% NP-40; containing 10µl/ml of protease inhibitor cocktail) on using an IKA Euro-ST D overhead stirrer (IKA-Werke GmbH, Staufen, Germany). Samples were then centrifuged (10 min at 10,000 *g*) and the protein content of the supernatants was then quantified with the Bradford assay using a SmartSpec Plus spectrophotometer (Bio-Rad Laboratories, Munich, Germany). Protein samples were normalized with a sample buffer (25 mM Tris-Cl, pH = 6.8, containing 1% SDS, 5% β-mercaptoethanol, 10% glycerol and 0.01% bromophenol blue), and 20 µg of protein from each sample were heated at 95ºC for 10 min, followed by electrophoresis separation in a 10% polyacrylamide gel (AppliChem GmBH, Darmstadt, Germany). Proteins were then transferred into a methanol-activated polyvinylidene difluoride (PVDF) membrane (Bio-Rad Laboratories). Non-specific binding sites were blocked with 5% low-fat powdered milk diluted in PBST (PBS + 0.25% Tween-20), and membranes were incubated overnight at 4ºC with anti-HSD11B2 antibody diluted at 1:250 in 2.5% low-fat powdered milk in PBST solution. Membranes were then incubated with a rabbit anti-guinea pig horseradish peroxidase (HRP)-conjugated antibody (1: 15000, A5545, Sigma Aldrich Chemie GmbH, Buchs, Switzerland), followed by the detection of signals with the SuperSignalWest Chemiluminescent Kit substrate (Thermo Fisher Scientific AG, Reinach, Switzerland) in a Chemi-Doc XRS+ System and Image Lab Software (Bio-Rad Laboratories). To ensure specificity, anti-HSD11B2 antibody was incubated for 1h at ambient temperature with the immunization peptide (blocking peptide) at the same dilution, before being used to blot the membrane. For loading control and relative quantification, PVDF membranes were re-blotted with mouse monoclonal antibody against ACTINB (1:1000, sc-69879, Santa Cruz Biotechnology, Santa Cruz, CA, USA), followed by a goat anti-mouse HRP-labelled secondary antibody (1: 15000, W402B, Promega). The optical density of bands was measured with ImageJ software (US National Institutes of Health, Bethesda, Maryland, USA). Relative protein expression was calculated by normalizing the optical density of HSD11B2 against ACTINB in the reblotted membranes and is presented as standardized optical density (SOD).

2.6 Evaluation of uteroplacental cortisol-cortisone conversion capacity

To evaluate the capacity of placental tissue to interconvert cortisol and cortisone, microsomal fractions (crude endoplasmic reticulum) were isolated from utero-placental sections collected during the post-implantation period, as well as from placenta and endometrium, and myometrial samples (macroscopically dissected) at the time of prepartum luteolysis (n = 4/group). This was done using the Endoplasmic Reticulum Isolation Kit (Sigma Aldrich Chemie GmbH), according to the manufacturer's directions and as previously described [49].

All conversion capacity assays were performed blinded, using incubation protocols modified after [49, 50]. Reaction mixtures (100 µl volume) were created by combining 50 µl of microsomal fractions with co-factors and substrates. For the cortisol to cortisone conversion assay, 0.25 mM NAD^+ (Roche Diagnostics, Mannheim, Germany) was used as co-factor, and substrate was 25 nM of unlabeled cortisol (Merk KGaA, Daarmstadt, Germany) and 1.82 nM (20 000 cpm) of tritium-labeled [1,2,6,7-3H(N)]-cortisol (PerkinElmer LAS GmbH, Rodgau, Germany). For the cortisone to cortisol conversion assay, the co-factor was 0.25 mM NADPH $+H^+$ (Roche Diagnostics), while the substrates were 25 nM of unlabeled cortisone (Merk KGaA) and 7.5 nM (60 000 cpm) of tritium-labeled [1,2-3H(N)]-cortisone (PerkinElmer LAS GmbH). The use of a mixture of unlabeled and 3H-labeled substrates was performed to minimize radioactive waste, while still allowing the evaluation of conversion rates. Mixtures using random samples were initially incubated for 0, 5, 10, 20 and 30 mins at 37ºC to determine the ideal incubation time. An incubation time of 20 mins was considered the most suitable time by showing the maximal conversion capacity of the mixture, and was then used for all subsequent experiments. After incubation was complete, samples were extracted with ethyl acetate, dried in a MicroDancer infrared vortex-evaporator (Hettich AG, Baech, Switzerland) and redissolved in 100 µl of HPLC mobile phase (methanol/acetonitrile/water 43:3:54 v/v/v). Samples were then separated via HPLC, following the protocol described in [51]. In short, 20 µl of dissolved extracts were separated on a 150 × 4 mm Eurospher II 100-5 C18 reversed-phase column in a Smartline Manager 5050 and Pump 150 HPLC system (all HPLC equipment from Knauer, Berlin, Germany) at a flow rate of 1 mL/min. Eluted fractions with 0.5 ml were then collected and evaporated. The 3H-activity in HPLC fractions was then measure by adding the scintillation cocktail Rotiszint eco plus (Carl Roth GmbH, Karlsruhe, Germany) in a Tri-Carb 2810 TR β-scintillation counter (PerkinElmer LAS GmbH). Differentiation between substrate and metabolite was based on a comparison of retention times with authentic tritiated standards. The percent of substrate conversion was calculated from the distribution of 3H activity among

the peaks after subtracting technical background of β-scintillation counter and baseline correction.

2.7 Statistical analysis

Statistical evaluation of changes in relative transcript levels (relative gene expression, RGE) and protein amounts (standardized optic density, SOD) between different stages of pregnancy was performed by one-way ANOVA, followed by Tukey-Kramer multiple comparisons post-test. In addition, two-tailed unpaired Student's t-test was performed to evaluated possible differences in pairwise comparisons, i.e. between mRNA amounts of *HSD11B1* and *-2* in different groups. The software GraphPad 2.06 (GraphPad Software Inc, San Diego, CA, USA) was used for this analysis and $P < 0.05$ was considered as statistically significant.

3. Results

3.1 Uterine/utero-placental gene expression during pregnancy

The transcriptional availability of *HSD11B1* and *-2* was evaluated in all uterine/utero-placental tissue samples. The mRNA availability of *HSD11B1* was significantly higher at mid-gestation, when compared with all earlier stages of pregnancy, and non-pregnant (E-) uterine samples ($P < 0.001$, Fig. 1A). There was a high variation in *HSD11B1* expression during luteolysis, yielding no significant difference between mid-gestation and luteolysis ($P > 0.05$, Fig. 1A). Yet, in antigestagen-induced luteolysis/abortion, the expression of *HSD11B1* was significantly increased 24 h after mid-pregnant animals were treated with aglepristone ($P < 0.05$, Fig. 1B). The availability of *HSD11B2* mRNA was the highest in post-implantation and mid-gestation samples, when compared with all other evaluated stages ($P < 0.05$, Fig. 1C). In contrast with *HSD11B1*, the expression of *HSD11B2* was downregulated in samples collected 24 and 72 h after aglepristone treatment ($P < 0.05$, Fig. 1D), resembling the pattern observed during normal luteolysis. In a pairwise comparison of both enzymes in canine uterine and utero-placental samples, *HSD11B2* expression was significantly higher than *-1* during post-implantation ($P < 0.001$, Fig. 1E). This changed during mid-gestation and prepartum luteolysis, with *HSD11B1* transcripts being more abundant than *HSD11B2* ($P < 0.01$ and $P < 0.05$, respectively, Fig. 1E). A higher expression of *HSD11B1* than *HSD11B2* was further observed in animals treated with aglepristone ($P < 0.01$, Fig. 1F).

3.2 Compartmentalization of *HSD11B1* and *-2* mRNA in the canine uterus

The mRNA abundance of all factors in different tissue layers, i.e., placental labyrinth, endometrium or myometrium, was assessed in utero-placental units collected during mid-gestation (i.e., in the mature fully developed placenta) and prepartum luteolysis. The availability of both *HSD11B1* and *HSD11B2* transcripts was frequently below detection limits in the myometrium of animals at mid-gestation resulting in the exclusion of these samples from the statistical evaluation. (Fig. 2). Due to high individual variability, no significant differences were observed for the expression of *HSD11B1* between the tissue compartments at mid-gestation ($P > 0.05$). This contrasted with its expression during prepartum luteolysis, with the placenta showing significantly higher levels than endometrium or myometrium ($P < 0.05$, Fig. 2A), suggesting the placenta as being the major source. *HSD11B2* transcripts were significantly more abundant in the mid-gestation placenta compared with mid-gestation endometrium ($P < 0.01$), and with the placental labyrinth and myometrium of prepartum luteolysis ($P < 0.001$ and $P < 0.01$, respectively, Fig. 2B). Furthermore, endometrial availability of *HSD11B2* was significantly higher than in the placenta during prepartum luteolysis ($P < 0.05$, Fig. 2B).

3.3 Protein expression of HSD11B2 in the canine utero-placental unit

The canine-specific anti-HSD11B2 antibody allowed the detection of a band close to the predicted protein size (44kDa) in western blot analysis (Fig. 3A). The signal was quenched with antibody pre-incubated with the immunization peptide (Fig. 3A). In utero-placental homogenates, HSD11B2 protein expression was significantly higher at post-implantation than mid-gestation and prepartum luteolysis ($P < 0.01$ and $P < 0.001$, respectively, Fig. 3B), mirroring the time-dependent changes observed at the mRNA level.

3.4 Localization of HSD11B1 and HSD11B2 in the canine placenta

The availability of custom-made anti-HSD11B2 antibody has made it possible to study its expression at both the protein and RNA level, whereas the localization of HSD11B1 was possible only by applying ISH.

During post-implantation, HSD11B2 was predominantly localized at the embryo-maternal interface of the developing placenta, in invading cytotrophoblast cells (Fig. 4A, left panels). In the mature placenta, during mid-gestation, signals were mostly localized in the syncytiotrophoblast, with some weaker staining in other cellular components (e.g. decidual cells or endothelial cells (Fig. 4A, center panels)). At prepartum luteolysis, the signals were weaker and a more diffuse staining pattern was observed (Fig. 4A, right panels). The

localization of HSD11B2-positive signals in the syncytiotrophoblast was then confirmed in the mature placenta by performing staining of consecutive slides (Fig. 4B) against PGR, as a marker of decidual cells [19, 20], and EDNRB, expressed by the syncytiotrophoblast [45].

With ISH, positive signals for *HSD11B1* were mostly localized in cytotrophoblast cells, with some signals also observed in maternal endothelial cells (Fig. 5A), while for *HSD11B2*, the signals were mainly observed in the syncytiotrophoblast, with a more diffuse pattern observed during luteolysis than during mid-gestation, as seen with IHC (Fig. 5B).

3.5 Enzymatic conversion between cortisol and cortisone in canine placental homogenates

The potential of the placenta to interconvert cortisol and cortisone was evaluated in samples collected during post-implantation, where a significantly higher mRNA availability of *HSD11B2* than *-1* was observed, and at the time of prepartum luteolysis, where an inverted pattern, associated with decreased protein expression of HSD11B2, was observed. Due to difficulties in the separation of intact tissue layers containing the invading trophoblast from remaining tissue layers in the still developing utero-placental interface at post-implantation, full tissue cross-sections were used for post-implantation specimens. On the other hand, in the fully developed placenta at prepartum luteolysis, the separation between physiological layers of placenta with adjacent endometrium from myometrium (the latter presenting low mRNA availability of both factors, being used as a negative control) was performed at the level of physiologically significantly enlarged endometrial chambers (i.e., deep endometrial glands). When evaluating conversion rates, values below 5% were considered as unreliable, as the presence of impurities or decay of the cortisol tracer, in addition to possible technical background of the beta counter, can mask weak conversion effects.

The conversion of cortisol into cortisone (i.e., inactivation of cortisol, indicating HSD11B2 activity), was significantly higher in utero-placental samples collected at post-implantation, when compared with the conversion rate observed with microsomes isolated from either the placenta or myometrium obtained during prepartum luteolysis ($P < 0.05$, Fig. 6). In contrast, the conversion of cortisone into cortisol (i.e., activation of cortisol) was undetected in post-implantation samples and myometrium from luteolysis, or remained below 1% in placental + endometrium samples collected during luteolysis (not shown).

4. Discussion

In the attempt to gain new insights into the utero-placental availability of cortisol in the dog, we evaluated the expression and localization of cortisol-to-cortisone interconverting enzymes

HSD11B1 and -2 in the canine uterus and utero-placental compartments throughout pregnancy. Both cortisol-regulating enzymes were expressed in all samples. Based on their significantly lower uterine expression at the pre-implantation stage (E+) and in corresponding non-pregnant controls (E-), as well as on the day of implantation (day 17), than in later gestational stages, they appeared to be predominantly associated with placental development and functionality. Therefore, subsequent analyses focused mainly on stages of pregnancy in which a placenta was present, i.e., post-implantation, mid-gestation and prepartum luteolysis. Indeed, *in situ* hybridization analysis of both factors, and immunohistochemical detection of HSD11B2, localized both enzymes predominantly to the fetal-derived trophoblast cells within the canine placental labyrinth.

The transcriptional availability of *HSD11B1* was the highest at mid-gestation, while *HSD11B2* mRNA levels were already increased during post-implantation. Therefore, there seemed to be a higher transcriptional availability of *HSD11B2* than *HSD11B1* associated with early placentation (post-implantation). An excessive exposure to glucocorticoids can cause detrimental effects in the establishment of pregnancy and in fetal development in different species [33, 52, 53]. Several of these effects are associated with disrupted expression of HSD11B2 [54, 55]. Thus, the cortisol-inactivating capacity of HSD11B2 has been characterized as a protective barrier against the passage of glucocorticoids into fetal circulation [33, 56-58]. In humans, e.g., fetal glucocorticoids are 5-10 times lower than maternal circulatory levels [59]. Although several studies have attempted to measure fetal exposition to cortisol in the dog using, e.g., puppy hair and claws [60, 61], a clear comparison with maternal levels is still not available. Nevertheless, it appears plausible that such a protective mechanism might be present in the dog, too. This hypothesis appears to be further supported by the microsomes activity assay, where an increased conversion of cortisol into cortisone was observed in post-implantation samples when compared with luteolysis. With regard to the post-implantation group, the high variability might be due to individual variations or to time-dependent changes. Nevertheless, there is a clearly higher capacity for cortisol inactivation (conversion to cortisone) during post-implantation than at the prepartum luteolysis. Within the fully developed fetal placental compartment, the strongest HSD11B2-positive signals were mainly localized in the syncytiotrophoblast. A similar localization pattern was previously described in mice, with placental HSD11B2 being mainly associated with the trophoblast [62], as well as in humans, where it was exclusively detected in the syncytiotrophoblast [58, 63]. Interestingly, in sheep, representing a non-invasive type of placentation, *HSD11B2* could be detected reliably in the trophectoderm and endoderm of the conceptus, but not in the uterus,

during early pregnancy [64]. Thus, despite the weak signals observed in endothelial and decidual cells in the present study, the increased cortisol-deactivation, possibly associated with a protective embryonal mechanism against maternal cortisol, appears to be mainly mediated by the trophoblast during early fetal development.

The progression of pregnancy towards parturition was associated with a decreased utero-placental expression of HSD11B2, which was confirmed at both the mRNA and protein levels. This was also reflected in its low activity at prepartum luteolysis based on the microsomal cortisol conversion rates. In fact, with average conversions of 2% in the placenta and endometrium, and 1.9% in myometrium (both below the defined 5% threshold), luteolysis appears to be virtually devoid of cortisol into cortisone conversion activity. The decreased placental availability of HSD11B2 at term was also highlighted by the assessment of mRNA in different utero-placental compartments, showing its significantly lowered levels between fully developed mid-term placenta and prepartum luteolysis. Fitting with these observations was the lowered *HSD11B2* transcription in antigestagen-treated dogs, emphasizing the P4-dependent expression of HSD11B2. This supports our previous report using the transcriptomic approach [30], where *HSD11B2* was described as a downstream factor from P4 signaling. As several samples used in the present work derived from previous projects, serum samples that could allow a correlation between placental expression of HSD11B1/2 and circulating cortisol or P4 were not available. Nevertheless, circulating P4 levels are described to a greater extent in the dog [s. reviewed in 65]. Thus, the time-dependent decrease of HSD11B2 expression appears to accompany, at least in part, the decreasing P4 circulating levels observed in this species, including the steep prepartum decline. In ovariectomized mouse, the uterine expression of *HSD11B2* could be upregulated by P4 administration, and later ablated by the PGR blocker mifepristone (RU486) [57]. Aglepristone used in our studies is a derivate of mifepristone, both type II antigestagens, with similarities in its chemical structure and activities related to the PGR [66]. Cumulatively, the recently postulated association between P4/PGR signaling and placental *HSD11B2* expression in the dog [30], is substantiated by the present findings, clearly indicating its importance in the luteolytic cascade.

The diffuse staining of HSD11B2 in the prepartum labyrinth could possibly be associated with its significantly lowered abundance and/or degradation. Conversely, the utero-placental availability of *HSD11B1* increased from post-implantation to mid-gestation, and remained unaffected at prepartum luteolysis. This was associated with an apparent shift in the transcriptional availability of both isoforms, with *HSD11B1* being significantly higher than -*2* at term. The ISH allowed the detection of mRNA encoding for *HSD11B1* mainly in the

cytotrophoblast, with some signals also identified in maternal endothelial cells during prepartum luteolysis These observations suggest that a possible interplay between the cortisol-deactivating syncytiotrophoblast and cortisol-activating cytotrophoblast could be present in the canine placenta. For instance, in mice, increased expression of *HSD11B1* can be observed in late pregnancy in fetal tissue [62], and in humans it is localized in endothelial cells and different trophoblast populations, but not in the syncytiotrophoblast [67]. As part of the approach involving microsomal activities, we investigated the potential of the placenta to activate cortisol, thereby addressing the activity of HSD11B1, which was below reliable detection limits in the placenta from prepartum luteolysis, and was undetectable in myometrium and in post-implantation samples. The inclusion of a positive control tissue, which was not possible in this study, could provide a more definitive answer regarding the lack of cortisol activation. While the low detection of HSD11B1 activity, and the limitations in protein detection, could be explained by a low availability of this enzyme in the canine placenta, this remains to be confirmed. The higher utero-placental transcriptional availability of *HSD11B1* in the antigestagen treated dogs differed from that observed during normal parturition. A possible explanation could be in the local stress-related response to acute PGR withdrawal [s. reviewed in 66]. Despite the still veiled importance of the parturition-associated increase of cortisol activity in the dog, as mentioned elsewhere, the cortisol-stimulated shift in placental steroidogenesis described for other species [1, 3], does not apply to the dog [14, 15]. Furthermore, only term, and not aglepristone-induced termination of pregnancy, was associated with the upregulation of GR/NR3C1 [29]. Nevertheless, the lower HSD11B2 activity appears to be associated with a locally increased availability of cortisol, possibly embryo-derived. This local cortisol increase could be an important event in the final maturation of the fetus, associated, e.g., with the final maturation of fetal organs, like the lung [68]. Still, the confirmation of such local events is still required, as previous cortisol measurements in the dog were performed at the circulating level [14, 23-25]. Furthermore, as already stated, termination of pregnancy in the dog is associated with increased circulating PGF2α levels, deriving from the trophoblast and involving the 9-keto PGE2 reductase (9KPGR)-mediated synthesis from PGE2 [49]. An interplay between PGF2α and cortisol has been described in several instances [1, 4]. However, the extent to which cortisol directly contributes to the placental PGF2α output affecting the synthetic cascade of prostaglandins in the dog, including the rising COX2/PTGS2 activity [21], remains to be investigated.

5. Conclusions

The results from the present work describe, for the first time, the presence of stage-dependent cortisol-modulating mechanisms in the canine placenta, mainly associated with the trophoblast. The higher expression of HSD11B2 in early placentation, associated with the local tissue potential to inactivate cortisol, might be involved in protective mechanisms of the embryo against maternal-derived glucocorticoids. The P4-dependent regulation of HSD11B2 is further substantiated by observation both during normal and induced parturition/abortion. A clear shift in placental regulation of cortisol activity is apparent at term, with parturition being associated with an increased *HSD11B1* mRNA availability, and decreased HSD11B2 expression and cortisol-inactivating activity. An interplay between different trophoblast populations is also apparent, with HSD11B1 being mainly localized in the cytotrophoblast, where GR/NR3C1 is also expressed [29], while HSD11B2-positive signals were mainly observed in the syncytiotrophoblast. Although its definitive role remains still to be defined for the dog, in accordance with our hypothesis, local cortisol appears to be involved in the termination of canine pregnancy and deserves more attention in the future.

Conflict of interests

The authors declare that they have no conflicts of interest.

Author's contributions

MTP was involved in developing the concept of the present study, experimental design, generating data, analysis and interpretation of data and drafting of the manuscript. GS was involved in the generation, analysis and interpretation of data, and revision of the manuscript. SA, RPC, IMR and KR were involved in the collection of tissue material, knowledge transfer, critical discussion and interpretation of data, and revision of the manuscript. MPK designed and supervised the project, was involved in interpretation of the data, and drafting and revision of the manuscript. All authors read and approved the final manuscript.

Acknowledgements

Authors are thankful to Dr. Sharon Mortimer for the careful editing of the manuscript. The technical expertise and contributions of Ricardo Fernandez Rubia and Kirstin Skaar are greatly appreciated. Part of the laboratory work was performed using the logistics at the Center for Clinical Studies, Vetsuisse Faculty, University of Zurich.

Figure legends

Figure 1. Relative gene expression of HSD11B1 and HSD11B2 in the canine uterus/utero-placental compartment during pregnancy and in response to antigestagens.

Relative gene expression is presented as determined by semi-quantitative real time (TaqMan) PCR ($\bar{X}$ +/- SD). **(A-D)** To evaluate the effects of pregnancy progression, or of preterm termination of pregnancy with aglepristone, one-way non-parametric ANOVA was applied, revealing: **(A)** $P < 0.0001$, **(B)** $P = 0.0197$, **(C)** $P < 0.0001$ and **(D)** $P = 0.0009$. When $P < 0.05$, analysis was followed by a Tukey-Kramer multiple comparison post-test. **(E, F)** Comparison of relative gene expression between *HSD11B1* and *HSD11B2* at each stage was evaluated by applying Student's unpaired two-tailed t- test. Bars with asterisks differ at: * $P < 0.05$, ** $P < 0.01$, *** $P < 0.001$. E- = embryo-negative/non-pregnant animals, E+ = embryo-positive/pre-implantation, day 17 = time of implantation, Post-Imp = post-implantation, Mid-Gest = mid-gestation.

Figure 2. Compartmentalization of HSD11B1 and HSD11B2 relative mRNA levels in the utero-placental tissue during mid-gestation and prepartum luteolysis. Relative gene expression, presented as $\bar{X}$ +/- SD, was determined by semi-quantitative real time (TaqMan) PCR. Samples from 3 animals for each pregnancy stage were used. Differences between all groups was assessed with one-way non-parametric ANOVA, with $P = 0.0079$ for HSD11B1 and $P < 0.0001$ for HSD11B1, followed by a Tukey-Kramer multiple comparison post-test. As the expression of both factors was frequently below detection limits in myometrium during mid-gestation, these samples were removed from statistical analysis. Bars with asterisks differ at: * $P < 0.05$, ** $P < 0.01$, *** $P < 0.001$.

Figure 3. Protein expression of HSD11B2 in utero-placental homogenates. (A) Epitope-blocking peptide was used to block HSD11B2-specific signal (~44kDa) in protein extract of utero-placental homogenates. **(B)** Representative immunoblots for HSD11B2 and ACTINB are shown. Standardized optical density (SOD) of HSD11B2 signals was measured in proteins extracted from utero-placental samples collected during post-implantation (Post-Imp), mid-gestation (Mid-Gest) and prepartum luteolysis. After quantifying HSD11B2 signals, membranes were re-blotted targeting ACTINB for normalization of signals intensity. SOD are presented as $\bar{X}$ +/- SD. One-way non-parametric ANOVA revealed $p = 0.0005$, followed by a Tukey-Kramer multiple comparison post-test.

Figure 4. Immunohistochemical localization of HSD11B2 in the canine placental labyrinth at selected stages of pregnancy. (A) During post-implantation, signals were observed in the invading trophoblast. In the mature mid-gestation placenta, strong positive signals were localized in syncytiotrophoblast cells, with weak signals also being observed in other placental cell populations (e.g. endothelial and decidual cells). Samples collected at the time of prepartum luteolysis appear to present a weaker and more diffuse pattern of staining. **(B)** The localization of HSD11B2-positive signals in the syncytiotrophoblast of the matured placenta was confirmed by performing consecutive staining of mid-gestation samples targeting PGR (expressed by decidual cells) and ETB (expressed by syncytiotrophoblast cells). No staining was observed in the isotype controls (insets in pictures, at the same magnification). Solid arrow = decidual cell; open arrow = endothelial cell; closed arrowhead = cytotrophoblast; open arrowhead = syncytiotrophoblast; asterisk = fetal stroma.

Figure 5. Localization of *HSD11B1* and *HSD11B2* mRNA in the canine placental labyrinth at mid-gestation and prepartum luteolysis. (A) *HSD11B1*-positive signals were mainly localized in cytotrophoblast and endothelial cells. Signal intensity in endothelial cells appeared to be stronger at prepartum luteolysis than at mid-gestation. (B) *HSD11B2* was mainly expressed in the syncytiotrophoblast during mid-gestation, with a more diffuse pattern being observed at the time of prepartum luteolysis. No staining was observed in the negative controls (sense probe; insets in pictures, at the same magnification). Open arrow = endothelial cell; closed arrowhead = cytotrophoblast; open arrowhead = syncytiotrophoblast.

Figure 6. Interconversion rate between cortisol and cortisone performed by canine utero-placental microsomes isolated from different stages of pregnancy. Microsome conversion rates of cortisol into cortisone are presented as a percentage. Differences between groups was assessed with one-way non-parametric ANOVA ($P = 0.0186$), followed by a Tukey-Kramer multiple comparison post-test. Bars with asterisks differ at: * $P < 0.05$.

5. References

1. Whittle, W.L., et al., *Glucocorticoid regulation of human and ovine parturition: the relationship between fetal hypothalamic-pituitary-adrenal axis activation and intrauterine prostaglandin production.* Biol Reprod, 2001. **64**(4): p. 1019-32.
2. Cottrell, E.C. and J.R. Seckl, *Prenatal stress, glucocorticoids and the programming of adult disease.* Front Behav Neurosci, 2009. **3**: p. 19.
3. Liggins, G.C., et al., *The mechanism of initiation of parturition in the ewe.* Recent Prog Horm Res, 1973. **29**: p. 111-59.
4. Schuler, G., R. Fürbass, and K. Klisch, *Placental contribution to the endocrinology of gestation and parturition.* Animal Reproduction, 2018. **15**(Suppl. 1): p. 822-842.

5. Tulchinsky, D., et al., *Plasma estrone, estradiol, estriol, progesterone, and 17-hydroxyprogesterone in human pregnancy. I. Normal pregnancy.* Am J Obstet Gynecol, 1972. **112**(8): p. 1095-100.
6. Heap, R.B. and R. Deanesly, *Progesterone in systemic blood and placentae of intact and ovariectomized pregnant guinea-pigs.* J Endocrinol, 1966. **34**(4): p. 417-23.
7. Mitchell, B.F. and M.J. Taggart, *Are animal models relevant to key aspects of human parturition?* Am J Physiol Regul Integr Comp Physiol, 2009. **297**(3): p. R525-45.
8. Nnamani, M.C., et al., *Evidence for independent evolution of functional progesterone withdrawal in primates and guinea pigs.* Evol Med Public Health, 2013. **2013**(1): p. 273-88.
9. Zakar, T. and F. Hertelendy, *Progesterone withdrawal: key to parturition.* Am J Obstet Gynecol, 2007. **196**(4): p. 289-96.
10. Ojasoo, T., et al., *Binding of steroids to the progestin and glucocorticoid receptors analyzed by correspondence analysis.* J Med Chem, 1988. **31**(6): p. 1160-9.
11. Philibert, D., et al., *From RU 38486 towards Dissociated Antiglucocorticoid and Antiprogesterone.* Frontiers of Hormone Research, 1991. **19**: p. 1-17.
12. Karalis, K., G. Goodwin, and J.A. Majzoub, *Cortisol blockade of progesterone: a possible molecular mechanism involved in the initiation of human labor.* Nat Med, 1996. **2**(5): p. 556-60.
13. Ogle, T.F. and B.K. Beyer, *Steroid-binding specificity of the progesterone receptor from rat placenta.* J Steroid Biochem, 1982. **16**(2): p. 147-50.
14. Hoffmann, B., et al., *Investigations on hormonal changes around parturition in the dog and the occurrence of pregnancy-specific non conjugated oestrogens.* Exp Clin Endocrinol, 1994. **102**(3): p. 185-189.
15. Nishiyama, T., et al., *Immunohistochemical study of steroidogenic enzymes in the ovary and placenta during pregnancy in the dog.* Anat Hist Embryol, 1999. **28**(2): p. 125-129.
16. Onclin, K., B. Murphy, and J.P. Verstegen, *Comparisons of estradiol, LH and FSH patterns in pregnant and nonpregnant beagle bitches.* Theriogenology, 2002. **57**(8): p. 1957-1972.
17. Kowalewski, M.P., et al., *The Dog: Nonconformist, Not Only in Maternal Recognition Signaling.* Adv Anat Embryol Cell Biol, 2015. **216**: p. 215-37.
18. Kowalewski, M.P., *Selected comparative aspects of canine female reproductive physiology*, in *Encyclopedia of Reproduction*, M.K. Skinner, Editor. 2018, Academic Press. p. 682-691.
19. Vermeirsch, H., P. Simoens, and H. Lauwers, *Immunohistochemical detection of the estrogen receptor-α and progesterone receptor in the canine pregnant uterus and placental labyrinth.* The Anatomical Record, 2000. **26**.
20. Kowalewski, M.P., et al., *Canine Endotheliochorial Placenta: Morpho-Functional Aspects.* Adv Anat Embryol Cell Biol, 2021. **234**: p. 155-179.
21. Kowalewski, M.P., et al., *Canine placenta: a source of prepartal prostaglandins during normal and antiprogestin-induced parturition.* Reproduction, 2010. **139**(3): p. 655-64.
22. Kowalewski, M.P., M. Tavares Pereira, and A. Kazemian, *Canine conceptus-maternal communication during maintenance and termination of pregnancy, including the role of species-specific decidualization.* Theriogenology, 2020. **150**: p. 329-338.
23. Concannon, P.W., et al., *Parturition and Lactation in the Bitch: Serum Progesterone, Cortisol and Prolactin.* Biology of Reproduction, 1978. **19**(5).
24. Veronesi, M.C., et al., *Correlations among body temperature, plasma progesterone, cortisol and prostaglandin F2alpha of the periparturient bitch.* J Vet Med A Physiol Pathol Clin Med, 2002. **49**(5): p. 264-8.
25. Olsson, K., et al., *Increased plasma concentrations of vasopressin, oxytocin, cortisol and the prostaglandin F2alpha metabolite during labour in the dog.* Acta Physiol Scand, 2003. **179**(3): p. 281-7.
26. Zone, M., et al., *Termination of pregnancy in dogs by oral administration of dexamethasone.* Theriogenology, 1995. **43**(2): p. 487-494.
27. Wanke, M., et al., *Clinical use of dexamethasone for termination of unwanted pregnancy in dogs.* J Reprod Fertil Suppl, 1997. **51**: p. 233-8.
28. Austad, R., A. Lunde, and O.V. Sjaastad, *Peripheral plasma levels of oestradiol-17 beta and progesterone in the bitch during the oestrous cycle, in normal pregnancy and after dexamethasone treatment.* J Reprod Fertil, 1976. **46**(1): p. 129-36.
29. Gram, A., et al., *Elevated utero/placental GR/NR3C1 is not required for the induction of parturition in the dog.* Reproduction, 2016. **152**(4): p. 303-11.
30. Nowak, M., et al., *Gene expression profiling of the canine placenta during normal and antigestagen-induced luteolysis.* Gen Comp Endocrinol, 2019. **282**: p. 113194.
31. Chapman, K., M. Holmes, and J. Seckl, *11beta-hydroxysteroid dehydrogenases: intracellular gate-keepers of tissue glucocorticoid action.* Physiol Rev, 2013. **93**(3): p. 1139-206.
32. Seckl, J.R. and B.R. Walker, *Minireview: 11beta-hydroxysteroid dehydrogenase type 1- a tissue-specific amplifier of glucocorticoid action.* Endocrinology, 2001. **142**(4): p. 1371-6.
33. Seckl, J.R. and M.J. Meaney, *Glucocorticoid programming.* Ann N Y Acad Sci, 2004. **1032**: p. 63-84.
34. Kowalewski, M.P., et al., *Luteal and placental function in the bitch: spatio-temporal changes in prolactin receptor (PRLr) expression at dioestrus, pregnancy and normal and induced parturition.* Reproductive Biology and Endocrinology, 2011. **9**(109).
35. Gram, A., A. Boos, and M.P. Kowalewski, *Uterine and placental expression of canine oxytocin receptor during pregnancy and normal and induced parturition.* Reprod Domest Anim, 2014. **49 Suppl 2**: p. 41-9.

36. Kowalewski, M.P., et al., *Time related changes in luteal prostaglandin synthesis and steroidogenic capacity during pregnancy, normal and antiprogestin induced luteolysis in the bitch.* Anim Reprod Sci, 2009. **116**(1-2): p. 129-38.
37. Graubner, F.R., et al., *Decidualization of the canine uterus: From early until late gestational in vivo morphological observations, and functional characterization of immortalized canine uterine stromal cell lines.* Reprod Domest Anim, 2017. **52 Suppl 2**: p. 137-147.
38. Concannon, P.W., J.P. McCann, and M. Temple, *Biology and endocrinology of ovulation, pregnancy and parturition in the dog.* J Reprod Fertil Suppl, 1989. **39**(0449-3087): p. 3-25.
39. Amoroso, E.C., *Placentation*, in *Marshall's Physiology of Reproduction*, A.S. Parkes, Editor. 1952, Longmans, Greens and Co: London, UK.
40. Tavares Pereira, M., et al., *Prostaglandin-mediated effects in early canine corpus luteum: in vivo effects on vascular and immune factors.* Reprod Biol, 2019. **19**(1): p. 100-111.
41. Kowalewski, M.P., et al., *Expression of cyclooxygenase 1 and 2 in the canine corpus luteum during diestrus.* Theriogenology, 2006. **66**(6-7): p. 1423-30.
42. Nowak, M., S. Aslan, and M.P. Kowalewski, *Determination of novel reference genes for improving gene expression data normalization in selected canine reproductive tissues - a multistudy analysis.* BMC Vet Res, 2020. **16**(1): p. 440.
43. Xie, F., et al., *miRDeepFinder: a miRNA analysis tool for deep sequencing of plant small RNAs.* Plant Molecular Biology, 2012. **80**(1): p. 75-84.
44. Nowak, M., et al., *Functional implications of the utero-placental relaxin (RLN) system in the dog throughout pregnancy and at term.* Reproduction, 2017. **154**(4): p. 415-431.
45. Gram, A., A. Boos, and M.P. Kowalewski, *Cellular localization, expression and functional implications of the utero-placental endothelin system during maintenance and termination of canine gestation.* 2017.
46. Kowalewski, M.P., et al., *Characterization of the canine 3beta-hydroxysteroid dehydrogenase and its expression in the corpus luteum during diestrus.* J Steroid Biochem Mol Biol, 2006. **101**(4-5): p. 254-62.
47. Tavares Pereira, M., et al., *Luteal expression of factors involved in the metabolism and sensitivity to oestrogens in the dog during pregnancy and in non-pregnant cycle.* Reprod Domest Anim, 2021.
48. Gram, A., et al., *Biosynthesis and degradation of canine placental prostaglandins: prepartum changes in expression and function of prostaglandin F2alpha-synthase (PGFS, AKR1C3) and 15-hydroxyprostaglandin dehydrogenase (HPGD).* Biol Reprod, 2013. **89**(1): p. 2.
49. Gram, A., et al., *Canine placental prostaglandin E2 synthase: expression, localization, and biological functions in providing substrates for prepartum PGF2alpha synthesis.* Biol Reprod, 2014. **91**(6): p. 154.
50. Li, X., et al., *Effects of Ziram on Rat and Human 11beta-Hydroxysteroid Dehydrogenase Isoforms.* Chem Res Toxicol, 2016. **29**(3): p. 398-405.
51. Turpeinen, U., et al., *Determination of urinary free cortisol by HPLC.* Clin Chem, 1997. **43**(8 Pt 1): p. 1386-91.
52. Jafari, Z., et al., *The Adverse Effects of Auditory Stress on Mouse Uterus Receptivity and Behaviour.* Sci Rep, 2017. **7**(1): p. 4720.
53. Li, Q.N., et al., *Glucocorticoid exposure affects female fertility by exerting its effect on the uterus but not on the oocyte: lessons from a hypercortisolism mouse model.* Hum Reprod, 2018. **33**(12): p. 2285-2294.
54. Rogers, S.L., et al., *Diminished 11beta-hydroxysteroid dehydrogenase type 2 activity is associated with decreased weight and weight gain across the first year of life.* J Clin Endocrinol Metab, 2014. **99**(5): p. E821-31.
55. Belkacemi, L., et al., *Altered placental development in undernourished rats: role of maternal glucocorticoids.* Reprod Biol Endocrinol, 2011. **9**: p. 105.
56. Togher, K.L., et al., *Epigenetic regulation of the placental HSD11B2 barrier and its role as a critical regulator of fetal development.* Epigenetics, 2014. **9**(6): p. 816-22.
57. Zheng, H.T., et al., *Progesterone-regulated Hsd11b2 as a barrier to balance mouse uterine corticosterone.* J Endocrinol, 2020. **244**(1): p. 177-187.
58. Zhu, P., et al., *Mechanisms for establishment of the placental glucocorticoid barrier, a guard for life.* Cell Mol Life Sci, 2019. **76**(1): p. 13-26.
59. Beitins, I.Z., et al., *The Metabolic Clearance Rate, Blood Production, Interconversion and Transplacental Passage of Cortisol and Cortisone in Pregnancy Near Term.* Pediatric Research, 1973. **7**(5): p. 509-519.
60. Fusi, J., et al., *The usefulness of claws collected without invasiveness for cortisol and dehydroepiandrosterone (sulfate) monitoring in healthy newborn puppies after birth.* Theriogenology, 2018. **122**: p. 137-143.
61. Groppetti, D., et al., *Maternal and neonatal canine cortisol measurement in multiple matrices during the perinatal period: A pilot study.* PLoS One, 2021. **16**(7): p. e0254842.
62. Thompson, A., V.K. Han, and K. Yang, *Spatial and temporal patterns of expression of 11beta-hydroxysteroid dehydrogenase types 1 and 2 messenger RNA and glucocorticoid receptor protein in the murine placenta and uterus during late pregnancy.* Biol Reprod, 2002. **67**(6): p. 1708-18.
63. Krozowski, Z., et al., *Immunohistochemical localization of the 11 beta-hydroxysteroid dehydrogenase type II enzyme in human kidney and placenta.* J Clin Endocrinol Metab, 1995. **80**(7): p. 2203-9.
64. Simmons, R.M., et al., *HSD11B1, HSD11B2, PTGS2, and NR3C1 expression in the peri-implantation ovine uterus: effects of pregnancy, progesterone, and interferon tau.* Biol Reprod, 2010. **82**(1): p. 35-43.
65. Kowalewski, M.P., *Luteal regression vs. prepartum luteolysis: regulatory mechanisms governing canine corpus luteum function.* Reprod Biol, 2014. **14**(2): p. 89-102.
66. Kowalewski, M.P., et al., *Progesterone receptor blockers: historical perspective, mode of function and insights into clinical and scientific applications.* Tierarztl Prax Ausg K Kleintiere Heimtiere, 2020. **48**(6): p. 433-440.

67. Sun, K., K. Yang, and J.R. Challis, *Differential expression of 11 beta-hydroxysteroid dehydrogenase types 1 and 2 in human placenta and fetal membranes.* J Clin Endocrinol Metab, 1997. **82**(1): p. 300-5.
68. Bolt, R.J., et al., *Glucocorticoids and lung development in the fetus and preterm infant.* Pediatr Pulmonol, 2001. **32**(1): p. 76-91.

Fig. 1

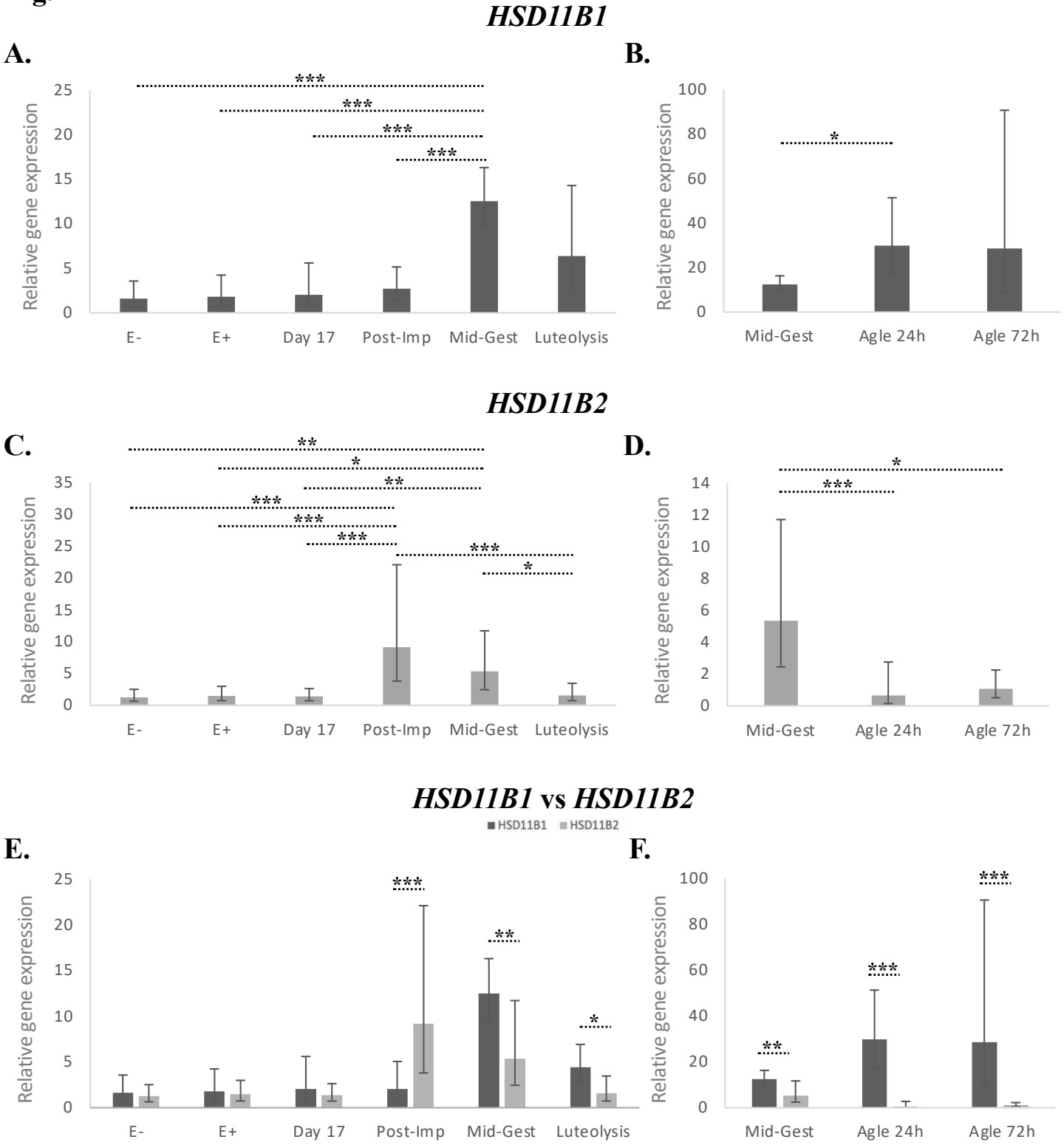
HSD11B1
A.
B.
Relative gene expression
E-
E+
Day 17
Post-Imp
Mid-Gest
Luteolysis
Agle 24h
Agle 72h
HSD11B2
C.
D.
HSD11B1 vs HSD11B2
E.
F.
HSD11B1
HSD11B2

Fig. 2

A. *HSD11B1*

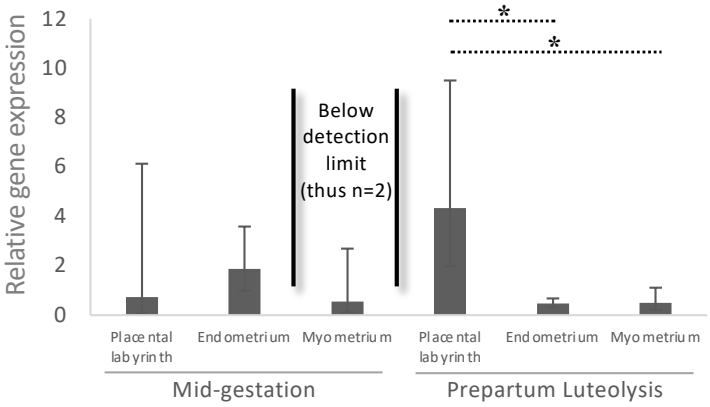

B. *HSD11B2*

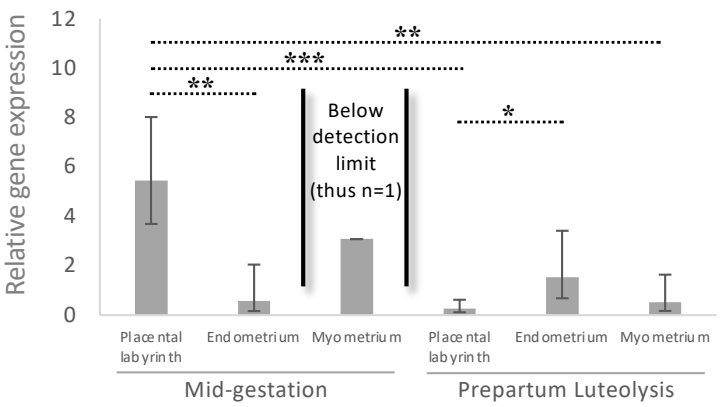

Fig. 3

A.


50 kDa
37 kDa
25 kDa
Anti-HSD11B2 antibody
Antibody + blocking peptides

B.

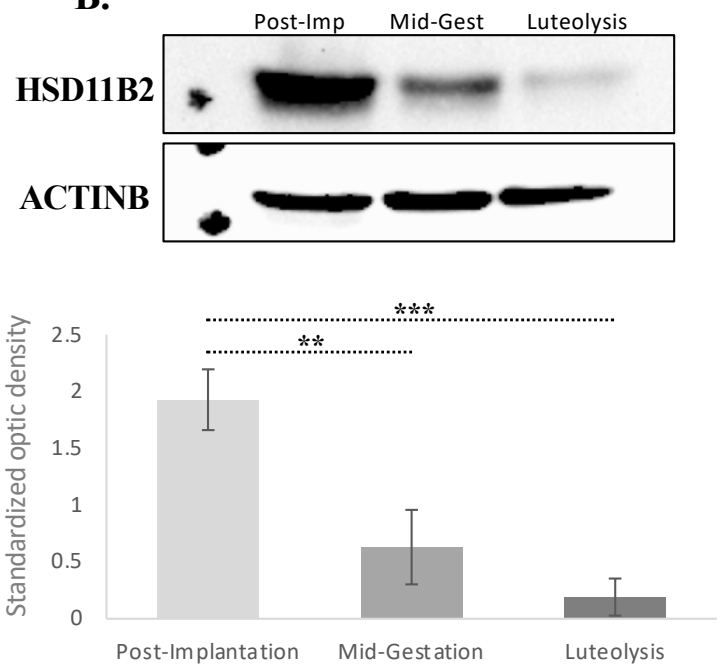
Post-Imp
Mid-Gest
Luteolysis
HSD11B2
ACTINB
***
**
Standardized optic density
2.5
2
1.5
1
0.5
0
Post-Implantation
Mid-Gestation
Luteolysis

Fig. 4

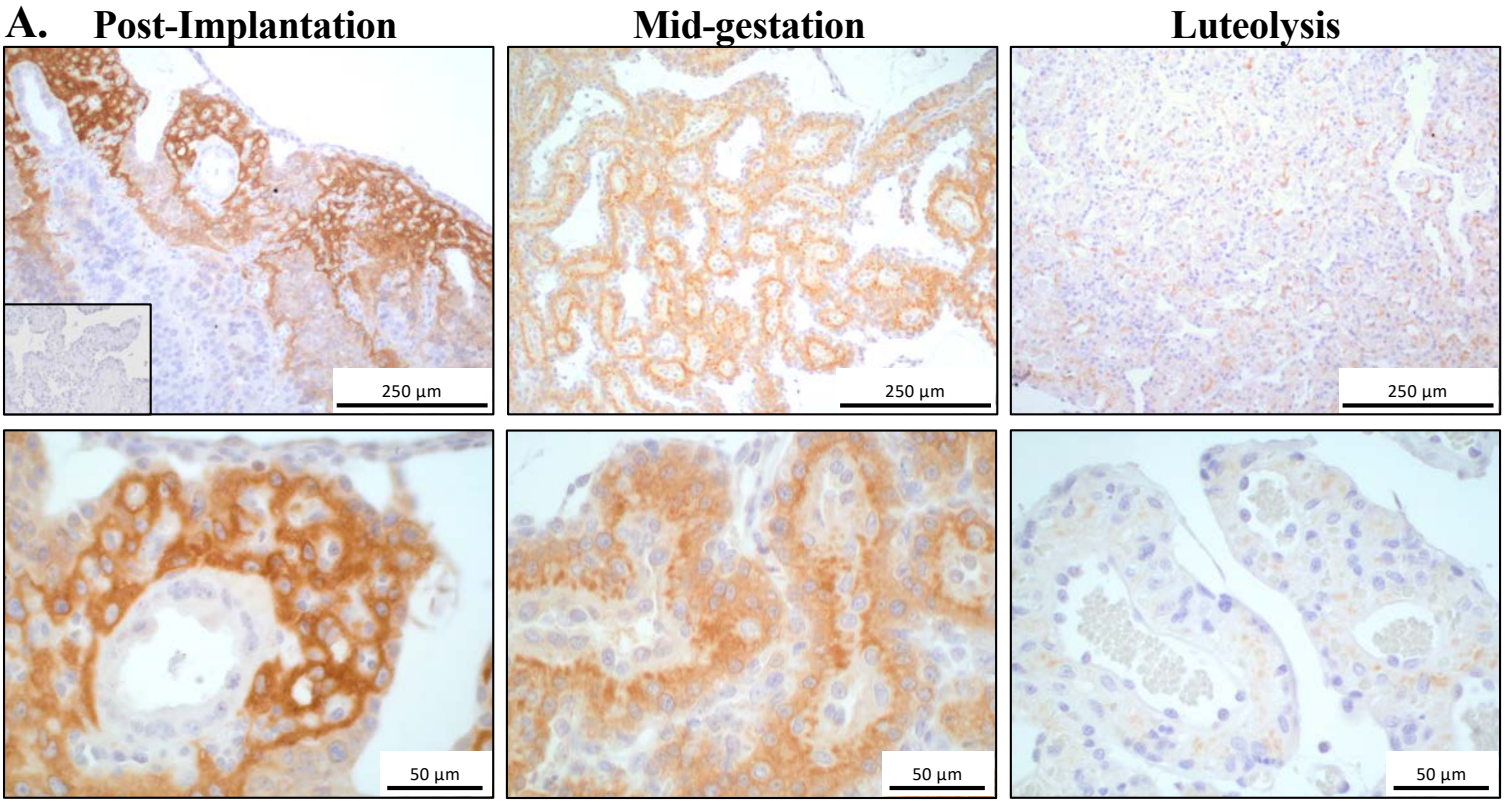
A.
Post-Implantation
Mid-gestation
Luteolysis
250 µm
250 µm
250 µm
50 µm
50 µm
50 µm

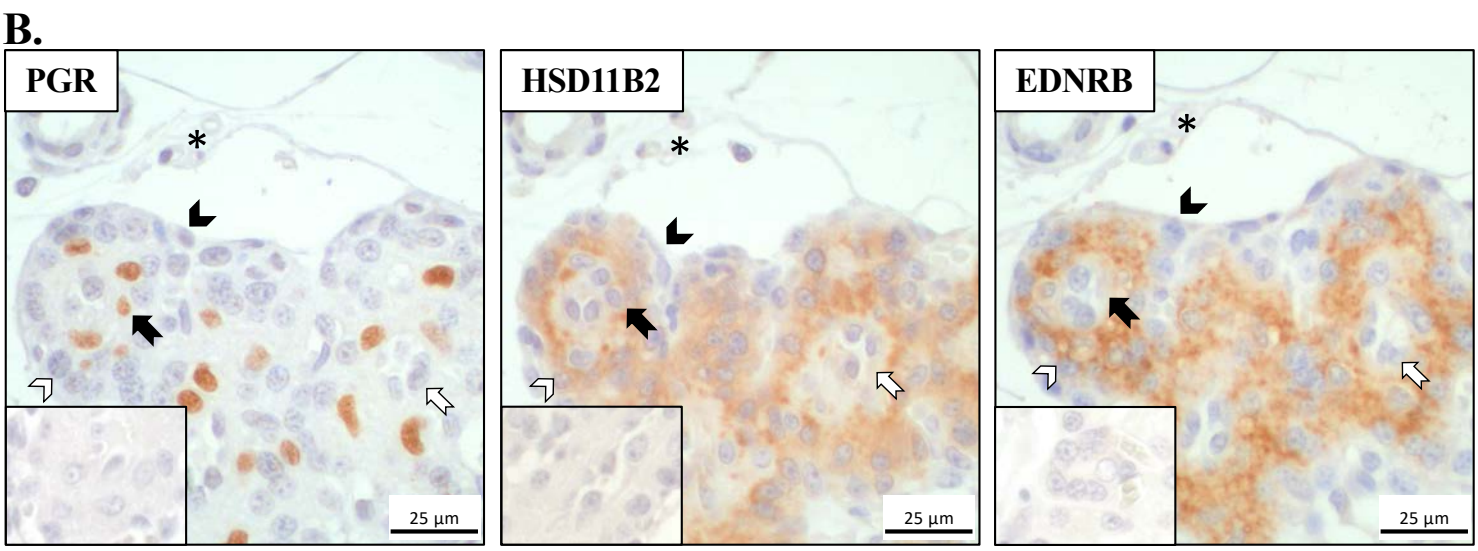
B.
PGR
HSD11B2
EDNRB
25 µm
25 µm
25 µm

Fig. 5

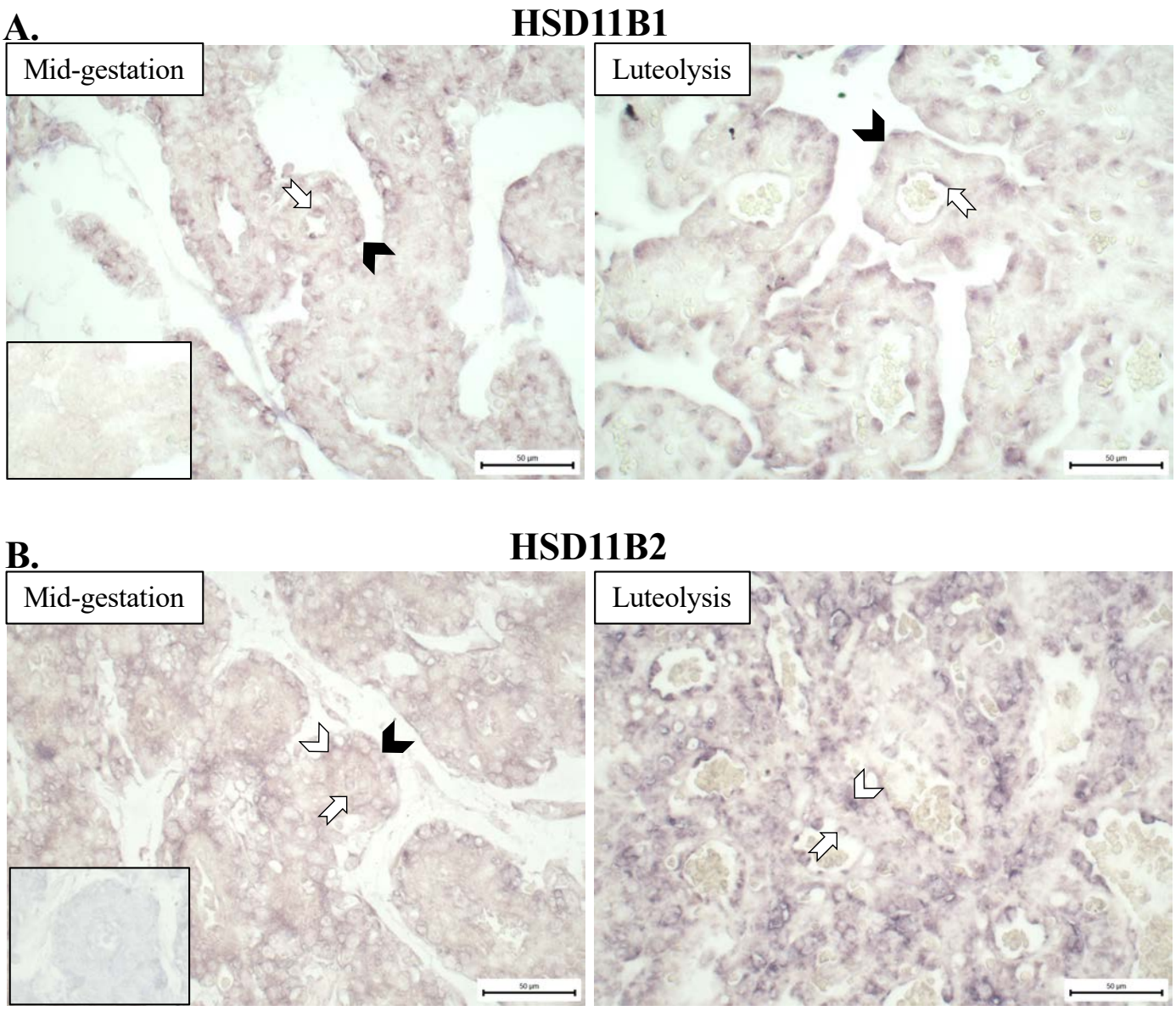
A.
HSD11B1
Mid-gestation
Luteolysis
B.
HSD11B2
Mid-gestation
Luteolysis

Fig. 6

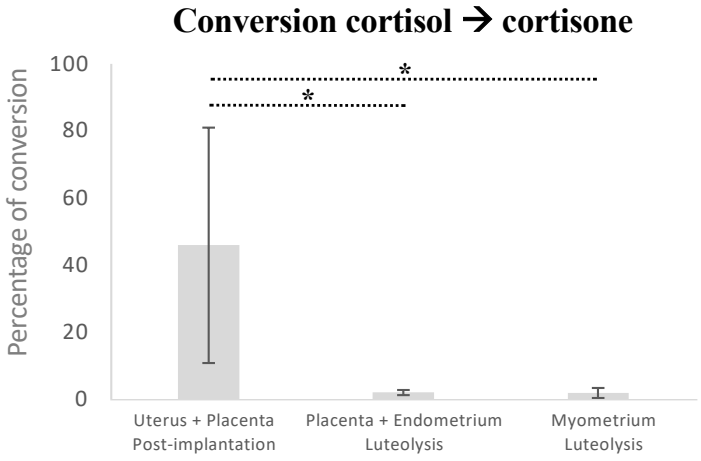
Conversion cortisol → cortisone
Percentage of conversion
100
80
60
40
20
0
*
*
Uterus + Placenta
Post-implantation
Placenta + Endometrium
Luteolysis
Myometrium
Luteolysis